

A Calabi–Yau Database

Threefolds Constructed from the Kreuzer–Skarke List

Ross Altman^a, James Gray^b, Yang-Hui He^{c,d,e}, Vishnu Jejjala^f, Brent D. Nelson^{a,g}

^aDepartment of Physics, Northeastern University, Boston, MA 02115, USA

^bPhysics Department, Robeson Hall, Virginia Tech, Blacksburg, VA 24061, USA

^cDepartment of Mathematics, City University, London, EC1V 0HB, UK

^dSchool of Physics, NanKai University, Tianjin, 300071, P.R. China

^eMerton College, University of Oxford, OX1 4JD, UK

^fCentre for Theoretical Physics, NITheP, and School of Physics,

University of the Witwatersrand, Johannesburg, WITS 2050, South Africa

^gICTP, Strada Costiera 11, Trieste 34014, Italy

Abstract

Kreuzer and Skarke famously produced the largest known database of Calabi–Yau threefolds by providing a complete construction of all 473,800,776 reflexive polyhedra that exist in four dimensions [1]. These polyhedra describe the singular limits of ambient toric varieties in which Calabi–Yau threefolds can exist as hypersurfaces. In this paper, we review how to extract topological and geometric information about Calabi–Yau threefolds using the toric construction, and we provide, in a companion online database (see <http://nuweb1.neu.edu/cydatabase>), a detailed inventory of these quantities which are of interest to physicists. Many of the singular ambient spaces described by the Kreuzer–Skarke list can be smoothed out into multiple distinct toric ambient spaces describing different Calabi–Yau threefolds. We provide a list of the different Calabi–Yau threefolds which can be obtained from each polytope, up to current computational limits. We then give the details of a variety of quantities associated to each of these Calabi–Yau such as Chern classes, intersection numbers, and the Kähler and Mori cones, in addition to the Hodge data. This data forms a useful starting point for a number of physical applications of the Kreuzer–Skarke list.

Contents

1	Introduction	1
2	Methods: Calabi–Yau Threefolds from Toric Construction	3
2.1	Kreuzer–Skarke Database	4
2.2	Parsing the Database using Sage	5
2.3	Stringy Hodge Numbers and Euler Number	5
2.4	MPCP Desingularization and Triangulation of Δ^*	5
2.5	Weight Matrix	8
2.6	The Chow Group and Intersection Numbers	10
2.7	Mori and Kähler Cones	13
2.8	Gluing of Kähler Cones	15
3	Querying the Database: Illustrative Examples	18
3.1	Search Fields	18
3.2	Search Results for General Calabi–Yau Properties	22
3.3	Search Results for Triangulation-Specific Calabi–Yau Properties	32
4	Discussion	40
A	Extended Glossary of Basic Terms	41
B	Nomenclature	46

1 Introduction

Calabi–Yau manifolds provide one of the simplest ways to compactify the extra dimensions of string theory while preserving some supersymmetry in four dimensions. Following the original idea of Kaluza and Klein [2,3], the topology and geometry of the extra dimensions determines the effective dynamics seen in the lower dimensional theory. Such geometrical constructions offer a rich framework for string phenomenology and more formal studies in a variety of different string theoretic contexts.

A compelling example of the use of Calabi–Yau threefolds in string theory can be seen in the subject of heterotic string phenomenology, as originally described in [4].¹ During the last decade, semi-realistic constructions exhibiting precisely the charged matter spectrum of the Standard Model of particle physics have been derived many times within this context [5–10]. The key point for this paper is that, given the link between geometry and low energy physics mentioned above, in all such

¹It should be emphasized that there is little consensus within the field as to which string theoretic construction is most likely to lead to realistic particle physics, with each approach having its own strengths and weaknesses.

discussions knowledge of the geometry of the Calabi–Yau threefolds involved is crucial in making progress.

Over the last three decades various large datasets of explicit constructions of Calabi–Yau manifolds have been developed, ranging from the so-called complete-intersection Calabi–Yau manifolds (CICYs) [11–17] to elliptically fibered manifolds over toric bases [18, 19] and hypersurfaces in toric ambient spaces [1, 20, 21]. By far the largest set found to date is given by the impressive work due to Kreuzer and Skarke in the 1990s: realizing Calabi–Yau threefolds as a hypersurfaces in four-dimensional toric varieties [1, 20]. A huge variety of different data sets have been isolated from this initial work. While all of the different applications are too numerous to list here, some interesting examples of such work can be found in these references [22–29].

Batyrev showed that a hypersurface in a toric variety can be chosen to be Calabi–Yau if the object underlying the construction of the variety, a lattice polytope, obeys the condition of reflexivity [30]. The classification of inequivalent reflexive polytopes is an exercise in combinatorics and is thus amenable to computer analysis. The software PALP (Package for Analyzing Lattice Polytopes) [31] was written with precisely this goal in mind. In all, an impressive 473,800,776 four-dimensional reflexive polytopes were found, each of which can be resolved to give candidate ambient spaces for Calabi–Yau threefold hypersurfaces.² Some important topological information such as the Hodge numbers for the Calabi–Yau associated to a given polytope can be found in the extremely useful website [32]. Here, and in the accompanying website [33], we wish to add to what can be found in [32], in order to fill a number of gaps in the information that is currently publicly available.

1. Although the number of distinct reflexive polytopes in the Kreuzer–Skarke database is well understood, it is unclear precisely how many distinct Calabi–Yau threefolds emerge from this list. Some of the geometrical data of these manifolds, such as Hodge numbers, can be determined purely in terms of the ambient polytope data. Of the 473,800,776 reflexive polytopes, it has been shown that there are 30,108 distinct pairs $(h^{1,1}, h^{2,1})$ counting the Kähler and complex structure moduli of the geometries respectively. However, different so-called triangulations into simplexes of the same polytope can potentially give rise to different Calabi–Yau hypersurfaces, which, while agreeing on this basic geometric data, differ in more subtle ways. In short, even taking into account the redundancy present in describing the same Calabi–Yau manifolds as hypersurfaces in different ambient spaces, there are likely to be many more than 473,800,776 Calabi–Yau threefolds in the Kreuzer–Skarke list. Unfortunately, performing all of the necessary triangulations to access this data is computationally intensive, and PALP is only able to complete the necessary computations for relatively low values of $h^{1,1}$ [34]. Clearly, therefore, it is of use to have as much of this data as possible pre-computed and archived in an easy-to-access format.
2. For calculations in subjects such as model building (for example in the heterotic case [35–37]), more than just the Hodge numbers of a Calabi–Yau threefold are required. The Chern classes, Kähler cones, and triple-intersection numbers, which help to characterize the Calabi–Yau

²For context, one might compare this to the case of two- and three-dimensional toric ambient spaces giving rise to Calabi–Yau one- and two-fold hypersurfaces (i.e., the torus and K3 surfaces). In these dimensions there are only 16 and 4,319 polytopes, respectively.

threefold in a more refined manner, are also needed, for example. These quantities can again be extracted from various versions, some not yet publicly available, of PALP. As in the previous bullet point, it is clear that we would like to have as much of this data as possible pre-computed and archived in an easy to access format.

3. A variety of codes are available for calculating geometrical properties of Calabi–Yau threefold hypersurfaces in toric varieties. Building upon the original work of Max Kreuzer and his collaborators, there have been some updated versions of PALP, consolidating and enhancing his contributions while providing additional documentation for the program [34,38]. In addition, new tools for analyzing such geometries are now available within the context of Sage [39] and TOPCOM [40]. In addition to being computationally intensive to run over large data sets, the language of programs such as PALP assume a level of detailed mathematical knowledge which, for physicists who are unfamiliar with the subject and simply wish to extract certain properties of the Calabi–Yau manifolds, may seem somewhat onerous to learn. Once more we see that it would be useful to have the data that physicists are interested in pre-computed and archived in a physicist’s language.

Given the above, our purpose in writing this paper is twofold. Firstly, we review the computational procedures for calculating the relevant topological and geometrical quantities of toric Calabi–Yau threefolds in a manner that is completely self-contained within the Sage computational package. Second, this paper supplies a user’s manual for how to quickly extract the Calabi–Yau data from the webpage [33], which provides an archive of this data in a pre-computed and easy-to-access format. Because of limitations in the computational power that has been applied to the problem to date, the database associated to this paper will provide all systematic triangulations up to $h^{1,1} = 6$ and provide partial results for $h^{1,1} = 7$. This already exceeds what be can be accessed with PALP, and importantly, the physicist accessing this data need not run or become familiar with any additional software. We expect to update the website as time goes by to accommodate ever increasing $h^{1,1}$.

The organization of this paper is as follows. For readers who are familiar with algebraic geometry but who have not studied toric varieties, we aim, in Section 2, to provide a pedagogical explanation of how practically to obtain geometrical data describing a Calabi–Yau threefold starting from an element of the dataset of [1,20]. Readers familiar with this subject should skip directly to Section 3, where we explain, with examples, how to extract a wide variety of information from the database of Calabi–Yau threefolds that we have derived from the Kreuzer–Skarke classification. Finally, we conclude with a discussion in Section 4. For the reader who is familiar with differential geometry but is not so comfortable with algebraic concepts, we provide in Appendix A a basic introduction to some of the notions which are used in the text. Finally, in Appendix B, we provide a glossary of the nomenclature used throughout this paper.

2 Methods: Calabi–Yau Threefolds from Toric Construction

In this section, we will review how to extract relevant topological and geometrical information about Calabi–Yau threefolds, starting from reflexive polytopes. Due to the work of Kreuzer and

Skarke [1, 32], not only do we know that the set of four-dimensional reflexive polytopes is finite, but we actually have a complete database of them to draw on. In the subsequent section we will present the results of using the methods we discuss here to convert the database of four-dimensional reflexive polytopes [32] to a database of Calabi–Yau threefold properties [33]. For a brief introduction to some of the key algebro-geometric concepts used in this section please refer to Appendix A.

In what follows, we will assume the ambient space \mathcal{A} to be a Gorenstein toric Fano variety with dimension $n = 4$ (although we will sometimes present results in general n) whose anticanonical divisor $X = -K_{\mathcal{A}}$ is a Calabi–Yau threefold hypersurface. As such, the Newton polytope Δ , corresponding one-to-one with \mathcal{A} is a reflexive polytope, which implies that Δ as well as its dual Δ^* are lattice polytopes containing only the origin in their respective interiors. Also, for simplicity of notation, we will represent all linear equivalence classes of divisors $[D]_{lin}$ by a representative divisor D . A more comprehensive explanation of our notation is provided in Appendix B.

2.1 Kreuzer–Skarke Database

Kreuzer and Skarke created an algorithm to generate all reflexive polytopes in dimension $n \geq 4$. Fortunately for us, we are only interested in dimension $n = 4$. It turns out that there are 473,800,776 reflexive polytopes with $n = 4$.

The output of the Kreuzer–Skarke (KS) database [32] is a text file with every 5 (i.e., $n + 1$) lines corresponding to a reflexive polytope. The first line is a summary of certain key information about the Newton polytope Δ , its dual Δ^* , and the toric variety \mathcal{A} they encode. It reads:

```
<dim( $\Delta$ )> <card( $\mathcal{V}(\Delta)$ )>
M:<card( $\Delta$ )> <card( $\mathcal{V}(\Delta)$ )>
N:<card( $\Delta^*$ )> <card( $\mathcal{V}(\Delta^*)$ )>
H:< $h^{1,1}(X), h^{2,1}(X)$ > [ $\chi(X)$ ]
```

Recall from Appendix B that the notation $\mathcal{V}(\Delta)$ represents the set of vertices of the reflexive polytope Δ , and $\text{card}(P)$ indicates the cardinality, or number of lattice points, in any subspace $P \subset M$ or N .

The remaining four (n) lines contain a matrix whose columns are the vertices $\mathbf{m} \in \mathcal{V}(\Delta)$ of the Newton polytope Δ . In this section, we will occasionally refer to the 95th polytope with $h^{1,1}(X) = 3$, $\Delta_{3,95}$ as an example. It is given in the KS database as:

```
4 6 M:100 6 N:8 6 H:3,81 [-156]
  1  1  1  1  -5  -5
  0  3  0  0  -6   0
  0  0  3  0   0  -6
  0  0  0  3  -3  -3
```

2.2 Parsing the Database using Sage

We first extract the necessary information from the database entry. The database directly gives us the vertices $\mathcal{V}(\Delta)$ of the Newton polytope. It also gives us the Hodge numbers $(h^{1,1}(X), h^{2,1}(X))$ and the Euler number $\chi(X)$ of a Calabi–Yau hypersurface $X \subset \mathcal{A}$, but we will recalculate these later for the sake of completeness.

`Sage` allows us to define the polytope Δ from vertices $\mathcal{V}(\Delta)$ using the `Polyhedron` class. The dual (or polar) polytope Δ^* can then be obtained using the `Polyhedron→polar()` method. From these, we can easily obtain the lattice points of Δ and Δ^* with `Polyhedron→integral_points()` as well as the vertices $\mathcal{V}(\Delta^*)$ with `Polyhedron→vertices()`.

We then obtain the faces $\mathcal{F}(\Delta)$ and $\mathcal{F}(\Delta^*)$ using the `Hypersurface` representation `Polyhedron→Hrepresentation()`. From this, it is a simple matter to construct the cones $\sigma_F = \text{cone}(F)$ using the `Cone` class. The cones of Δ and Δ^* can each be joined into fans $\Sigma(\Delta)$ and $\Sigma(\Delta^*)$ using the `Fan` class.

2.3 Stringy Hodge Numbers and Euler Number

The stringy Hodge numbers for a generic Calabi–Yau hypersurface $X \subset \mathcal{A}$ can be computed using Batyrev’s well-known formulae [30] :

$$\begin{aligned}
 h^{1,1}(X) &= \text{card}(\Delta^*) - 5 - \sum_{\text{codim}(F^*)=1} \text{card}(\text{relint}(F^*)) + \sum_{\text{codim}(F^*)=2} \text{card}(\text{relint}(F^*)) \cdot \text{card}(\text{relint}(F)) \\
 h^{2,1}(X) &= \text{card}(\Delta) - 5 - \sum_{\text{codim}(F)=1} \text{card}(\text{relint}(F)) + \sum_{\text{codim}(F)=2} \text{card}(\text{relint}(F)) \cdot \text{card}(\text{relint}(F^*)). \tag{2.1}
 \end{aligned}$$

The Euler number is then easily computed via

$$\chi(X) = 2 \cdot (h^{1,1}(X) - h^{2,1}(X)). \tag{2.2}$$

2.4 MPCP Desingularization and Triangulation of Δ^*

The variety \mathcal{A} generated by Δ may be a singular space. If it is too singular, then our Calabi–Yau hypersurface $X \subset \mathcal{A}$ may not be smooth even though it is base point free. Therefore, we must find an appropriate resolution of singularities given by a birational morphism $\pi : \tilde{\mathcal{A}} \rightarrow \mathcal{A}$ such that the desingularized space $\tilde{\mathcal{A}}$ is smooth enough that the hypersurface $X \subset \tilde{\mathcal{A}}$ can be chosen smooth. Because X has dimension 3, it can generically be transversally (i.e., smoothly) deformed around singular loci with codimension 3. Such singular loci with codimension ≥ 3 are called *terminal singularities* [41]. Thus, we need only consider partial desingularizations which resolve everything up to terminal singularities.

Another important condition for X to be smooth is for it to be well-defined everywhere when viewed as a Cartier divisor. For this to be true, we must be able to write X uniquely in terms of a basis on every coordinate patch U on the open cover of $\tilde{\mathcal{A}}$. Because an ample (effective) Cartier

divisor is defined locally on U by a single regular function, this means that the regular functions on U must form a unique factorization domain. When $\tilde{\mathcal{A}}$ is smooth, all ample divisors are Cartier, and we say that $\tilde{\mathcal{A}}$ is *factorial*. However, if $\tilde{\mathcal{A}}$ contains terminal singularities (i.e. is quasi-smooth), an ample divisor may only be \mathbb{Q} -Cartier. In this case, we say that $\tilde{\mathcal{A}}$ is *\mathbb{Q} -factorial*. A variety with only terminal singularities is already a normal variety, so that the regular functions on U are integrally closed, however \mathbb{Q} -factoriality is a stronger condition. A hypersurface in a variety of this kind will be smooth [42]

Because reflexive polytopes correspond one-to-one with birational equivalence classes of Gorenstein toric Fano varieties, we are guaranteed that $X = -K_{\mathcal{A}}$ is already ample, and so we need not introduce any exceptional divisors (discrepancies) to the canonical divisor in the desingularization π , i.e., $K_{\tilde{\mathcal{A}}} = \pi^*(K_{\mathcal{A}})$, and we say that the desingularization is *crepant* [30, 43]. As a result, the desingularized space $\tilde{\mathcal{A}}$ will still be a Gorenstein toric Fano variety, and therefore projective.

Following Batyrev [30], we define a *maximal projective crepant partial (MPCP) desingularization* $\pi : \tilde{\mathcal{A}} \rightarrow \mathcal{A}$ to be one such that the pullback π^* is crepant, and the desingularized space $\tilde{\mathcal{A}}$ is \mathbb{Q} -factorial and has no worse than terminal singularities. Furthermore, given any Gorenstein toric Fano variety \mathcal{A} , there exists at least one such MPCP desingularization π (see [30] for the proof).

More importantly for our purposes is how this desingularization is reflected in the polytope formulation. The removal of non-terminal singularities can be approached by refining the open cover $\mathcal{U}(\tilde{\mathcal{A}})$ on $\tilde{\mathcal{A}}$ as much as possible. Because each maximal 4-cone of Δ^* corresponds to a coordinate patch $U \in \mathcal{U}(\tilde{\mathcal{A}})$, this amounts to subdividing the maximal cones as much as possible such that each subdivision is still a convex rational polyhedral cone with a vertex at the origin. We call this a *fine, star subdivision* with *star center* at the origin. The condition of \mathbb{Q} -factoriality requires that each new subdivided maximal cone is *simplicial*, i.e., each has four generating rays (since we require $n = 4$).

This kind of subdivision is in fact a *triangulation* into simplexes. Also, because $\tilde{\mathcal{A}}$ must be projective, these simplicial cones must be projections of cones from an embedding space. In the literature, these are referred to as *regular triangulations* [44–46]. Thus, in order to find an MPCP desingularization for \mathcal{A} , we must find at least one fine, star, regular triangulation (FSRT) of Δ^* .

Before we move on, there is an important point to be made here. All lattice points other than the origin are either vertices $\mathcal{V}(\Delta^*)$, or they are not $\hat{\mathcal{V}}(\Delta^*) = \Delta^* \setminus \mathcal{V}(\Delta^*)$. Because Δ^* is reflexive and therefore contains no interior points save the origin, it must be true that both $\mathcal{V}(\Delta^*), \hat{\mathcal{V}}(\Delta^*) \subset \partial\Delta^*$. Before desingularization, the generating rays of the maximal cones $\sigma \in \Sigma_4(\Delta^*)$ are the minimal cones $\sigma \in \Sigma_1(\Delta^*)$ whose lattice points include only the origin and points in $\mathcal{V}(\Delta^*)$. But, the notion of subdivision of maximal cones implies that before desingularization, $\hat{\mathcal{V}}(\Delta^*) \neq \emptyset$. In general, this is true; for each facet $F \in \mathcal{F}_3(\Delta^*)$, there may be lattice points on the boundary such that $\text{skel}_2(\Delta^*) \supset \partial F \neq \emptyset$ and there may be points in the interior such that $\text{skel}_3(\Delta^*) \supset \text{relint}(F) \neq \emptyset$. However, in the case that $\tilde{\mathcal{A}}$ has only terminal singularities, we may ignore points in $\text{relint}(F)$ in the process of subdivision.

This can be explained by considering the orbifold group on $\tilde{\mathcal{A}}$, whose construction is given by [29]

$$\tilde{G} \cong N/\Lambda_{n-1} \tag{2.3}$$

where Λ_d is the lattice generated by $\text{skel}_d(\Delta^*)$. We now apply an important result of Hasse and Nill [47]:

$$\text{if } n \geq 3, \quad \Lambda_{n-2} = \Lambda_{n-1}. \quad (2.4)$$

Since we are working with $n = 4$, this result implies that $\Lambda_2 = \Lambda_3$, and the orbifold group depends only on Λ_2 . Therefore, we may effectively ignore points which appear in $\text{skel}_3(\Delta^*)$ and not in $\text{skel}_2(\Delta^*)$.

The underlying reason for this is that with Δ^* reflexive, these points interior to facets correspond precisely to the Demazure roots [29, 47–49] for the orbifold automorphism group \tilde{G} . Thus, to maximize computational efficiency, we need only triangulate the point configuration $\text{skel}_2(\Delta^*)$.

In practice, we want this point configuration to be searchable, so we choose the specific ordering of points given by

$$\mathcal{P}(\Delta^*) = \text{sort}(\mathcal{V}(\Delta^*)) \cup \text{sort}(\text{skel}_2(\Delta^*) \setminus \mathcal{V}(\Delta^*)). \quad (2.5)$$

Effectively, then, subdivision of the fan will correspond to expanding the set of vertices of Δ^* from $\mathcal{V}(\Delta^*)$ to $\mathcal{P}(\Delta^*)$. We will sometimes refer to the points in $\mathcal{P}(\Delta^*)$ (or just \mathcal{P}) as the *resolved vertices* of Δ^* . Furthermore, vertices $\mathbf{n}_\rho \in \mathcal{P}$ correspond one-to-one with toric divisors $D_\rho \subset \tilde{\mathcal{A}}$ with bijection $\mathbf{n}_\rho \rightarrow D_\rho$.

It is possible to enumerate the FSRTs of the configuration \mathcal{P} (with star center at the origin) using TOPCOM [40, 50], however, this becomes highly inefficient as $\text{card}(\mathcal{P})$ becomes large. A better way to proceed, which is also inherently parallelizable, is to instead consider the configurations $\mathcal{P} \cap \sigma$ for each $\sigma \in \Sigma_4(\Delta^*)$. The FSRTs of each maximal cone σ can then be obtained separately, each using Volker Braun’s tremendously useful implementation of TOPCOM in Sage, and then recombined. For each maximal cone, TOPCOM returns a set

$$\mathcal{T}(\mathcal{P} \cap \sigma) = \{T_\sigma \mid T_\sigma \text{ an FSRT of } \mathcal{P} \cap \sigma\}. \quad (2.6)$$

The trade-off for computation efficiency here is that the recombination of triangulated maximal cones is somewhat intricate and tricky. We use the following algorithm^{3,4}:

1. Choose a triangulation $T_\sigma \in \mathcal{T}(\mathcal{P} \cap \sigma)$ for each maximal cone $\sigma \in \Sigma_4(\Delta^*)$.
If all combinations have previously been checked, terminate.
2. Split up all maximal cones into pairs (σ, σ') (if there is an odd number, there will be one unpaired cone).
3. For one pair (σ, σ') , check that:
 - For each simplex $S \in T_\sigma$, there exists a simplex $S' \in T_{\sigma'}$ such that $S \cap S' \cap \sigma \cap \sigma' \neq \emptyset$.
 - For each simplex $S' \in T_{\sigma'}$, there exists a simplex $S \in T_\sigma$ such that $S \cap S' \cap \sigma \cap \sigma' \neq \emptyset$.
 - $T_\sigma \cup T_{\sigma'}$ is a regular triangulation (see below).

³We would like to thank Volker Braun for suggesting to us this method of parallelization via the triangulation of maximal cones.

⁴A similar algorithm was in use concurrently by Long, McAllister, and McGuirk (see [51]).

True if (σ, σ') satisfies all conditions, false otherwise.

- If true, repeat step 3 for the next pair.
 - If false, repeat step 1 with a different combination of triangulations $T_\sigma \in \mathcal{T}(\mathcal{P} \cap \sigma)$ for each maximal cone $\sigma \in \Sigma_4(\Delta^*)$.
4. • If there is only one pair (σ, σ') , then the triangulation $T = T_\sigma \cup T_{\sigma'}$ is an FSRT of \mathcal{P} , and therefore of Δ^* (i.e., $T \in \mathcal{T}(\mathcal{P})$).
Repeat step 1 with a different combination of triangulations $T_\sigma \in \mathcal{T}(\mathcal{P} \cap \sigma)$ for each maximal cone $\sigma \in \Sigma_4(\Delta^*)$.
- Otherwise, define new cones and triangulations by combining each pair via $\tilde{\sigma} = \sigma \cup \sigma'$ and $T_{\tilde{\sigma}} = T_\sigma \cup T_{\sigma'}$.
Split up all new cones into pairs $(\tilde{\sigma}, \tilde{\sigma}')$ and repeat step 3.

To check whether a triangulation T of the point set \mathcal{P} is regular, we use the following well-known algorithm [45, 46, 52]

1. Compute the Gale transform⁵ \mathcal{P}^\vee of \mathcal{P} .
2. For each simplex $S \in T$, define the set $\mathcal{Q}(S) = \{\mathbf{n}_i^\vee \in \mathcal{P}^\vee \mid \mathbf{n}_i \in \mathcal{P} \setminus S\}$.
3. If $\bigcap_{S \in T} \text{relint}(\text{cone}(\mathcal{Q}(S))) \neq \emptyset$, then T is a regular triangulation of \mathcal{P} .

2.5 Weight Matrix

Recall from equation (A.5) the definition of a toric variety

$$\mathcal{A} \cong \frac{V}{(\mathbb{C}^*)^{k-n} \times G}. \quad (2.7)$$

After desingularization, we obtain a similar toric variety given by

$$\tilde{\mathcal{A}} \cong \frac{\tilde{V}}{(\mathbb{C}^*)^{k-n} \times \tilde{G}}. \quad (2.8)$$

The group \tilde{G} is nothing more than the orbifold group $\tilde{G} = N/\Lambda_{n-1}$. However, we must still describe the action on $\tilde{\mathcal{A}}$ of the split $(k-n)$ -torus $(\mathbb{C}^*)^{k-n}$ given by the product of 1-tori \mathbb{C}^* .

The toric variety $\tilde{\mathcal{A}}$ may be treated as a weighted projective space with respect to each of the $k-n$ split 1-tori \mathbb{C}^* with weights $\mathbf{w}_r = (w_r^1, \dots, w_r^k) \in (\mathbb{Z}_{\geq 0})^k$ such that

$$(z_1, \dots, z_k) \sim (\lambda^{w_r^1} z_1, \dots, \lambda^{w_r^k} z_k), \quad \lambda \in \mathbb{C}^*, \quad (2.9)$$

for all $r = 1, \dots, k-n$ running over the 1-tori.

⁵The Gale transform \mathcal{P}^\vee of a set of points \mathcal{P} is given by constructing the set of augmented vectors $\hat{\mathcal{P}} = \{(1, \mathbf{n}) \mid \mathbf{n} \in \mathcal{P}\}$, and solving the matrix equation $[\hat{\mathcal{P}}] \cdot [\mathcal{P}^\vee]^T = \mathbf{0}$.

It can be shown that the weights w_r^ρ satisfy an equation of the form

$$\sum_{\rho=1}^k w_r^\rho \cdot \langle \mathbf{m}, \mathbf{n}_\rho \rangle = 0, \forall \mathbf{m} \in \Delta, \quad (2.10)$$

or because the fan $\Sigma(\Delta)$ is complete, we can equivalently write

$$\sum_{\rho=1}^k w_r^\rho \mathbf{n}_\rho = \mathbf{0}. \quad (2.11)$$

Recall that for $\tilde{\mathcal{A}}$, the vertices of Δ^* are given by $\mathbf{n}_\rho \in \mathcal{P}$ such that $k = \text{card}(\mathcal{P})$. Then, equation (2.11) can be written in matrix form such that

$$[\mathcal{P}] \cdot \mathbf{W}^T = \mathbf{0} \quad \text{with} \quad \sum_{\rho=1}^k w_r^\rho > 0 \quad \text{and} \quad \mathbf{W} \geq 0, \quad (2.12)$$

where \mathbf{W} is the $(k-n) \times k$ weight matrix

$$\mathbf{W} = \begin{pmatrix} \mathbf{w}_1 \\ \vdots \\ \mathbf{w}_{k-n} \end{pmatrix} = \begin{pmatrix} w_1^1 & \cdots & w_1^k \\ \vdots & \ddots & \vdots \\ w_{k-n}^1 & \cdots & w_{k-n}^k \end{pmatrix}. \quad (2.13)$$

Thus, we see that

$$\mathbf{w}_1, \dots, \mathbf{w}_{k-n} \in \ker([\mathcal{P}]) \text{ linearly independent.} \quad (2.14)$$

where we assume the kernel to be taken over the integers, so that the weights are well-defined as exponents in a polynomial.

The kernel $\ker([\mathcal{P}])$ can be easily computed in **Sage** given \mathcal{P} . However, in general, non-negativity of the entries of \mathbf{W} is not guaranteed this way. We overcome this limitation by restricting to the positive orthant $(\mathbb{Z}_{\geq 0})^k$, such that

$$\mathbf{w}_1, \dots, \mathbf{w}_{k-n} \in \ker([\mathcal{P}]) \cap (\mathbb{Z}_{\geq 0})^k \text{ linearly independent.} \quad (2.15)$$

To perform this computation in **Sage**, we create two **Polyhedron** objects, one generated by *lines* specified by the elements of $\ker([\mathcal{P}])$, and the other generated by *rays* specified by the unit basis vectors:

```
sage: kerPolyhedron = Polyhedron(lines=ker.basis());
sage: posOrthant = Polyhedron(rays=identity_matrix(ker.ngens()).columns());
```

The rays of the intersection of these objects are guaranteed to be non-negative, however there may be redundant elements. Because there are $k-n$ tori, we should find that $\text{rank}(\mathbf{W}) = k-n$. Again, in the interest of organization, we sort the elements in ascending order and choose the first $k-n$ linearly independent ones. These will be the rows of the weight matrix \mathbf{W} .

2.6 The Chow Group and Intersection Numbers

Next, we review how to compute the Chow group $A^1(\tilde{\mathcal{A}})$, which describes the intersection of divisors on $\tilde{\mathcal{A}}$. Recall from Appendix A that the Chow group of Cartier divisors is given by the quotient $A^1(\tilde{\mathcal{A}}) \cong \mathcal{C}(\tilde{\mathcal{A}}) / \sim_{lin}$. We will therefore need to work out the ideal which generates linear equivalence classes among the divisors.

2.6.1 Linear Ideal and Stanley–Reisner Ideal

There is an analogous equation to (2.11), the defining equation of the weight matrix, relating toric divisors. It can be written

$$\sum_{\rho=1}^k \mathbf{n}_\rho \cdot D_\rho = \mathbf{0}. \quad (2.16)$$

This gives a linear relation between the divisors and we define the *linear ideal*

$$I_{lin} = \sum_{\rho=1}^k \mathbf{n}_\rho \cdot D_\rho. \quad (2.17)$$

In addition, there are non-linear relationships among the toric divisors. Consider a case where we have d toric divisors such that $D_{i_1} \cdot \dots \cdot D_{i_d} = \int_{\tilde{\mathcal{A}}} \gamma(D_{i_1}) \wedge \dots \wedge \gamma(D_{i_d}) = 0$. In the polytope construction, these divisors with null intersection correspond to the points $\mathbf{n}_{i_1}, \dots, \mathbf{n}_{i_d} \in \mathcal{P}$ which do not appear together as vertices of any simplex $S \in T(\tilde{\mathcal{A}})$ in the FSRT $T(\tilde{\mathcal{A}})$ corresponding to the MPCP desingularization $\tilde{\mathcal{A}}$. The set of these null intersections forms another ideal

$$I_{SR}(\tilde{\mathcal{A}}) = \{D_{i_1} \cdot \dots \cdot D_{i_d} \mid \mathbf{n}_{i_1}, \dots, \mathbf{n}_{i_d} \notin S, \forall S \in T(\tilde{\mathcal{A}})\} \quad (2.18)$$

known as the *Stanley–Reisner ideal*. These sets of divisors with null intersections clearly provide another constraint on the Chow group of intersections.

2.6.2 Chow Group

Given I_{lin} and $I_{SR}(\tilde{\mathcal{A}})$, we have all the information we need to define linear equivalence classes between the Cartier divisors in $\mathcal{C}(\tilde{\mathcal{A}})$. Then, we are in a position to define the Chow group as the quotient

$$A^1(\tilde{\mathcal{A}}) \cong \frac{\mathcal{C}(\tilde{\mathcal{A}})}{I_{lin} + I_{SR}(\tilde{\mathcal{A}})}. \quad (2.19)$$

In practice, we do not know what $\mathcal{C}(\tilde{\mathcal{A}})$ is. However, the Picard group of a toric variety is given by $\text{Pic}(\tilde{\mathcal{A}}) \cong \mathbb{Z}^{k-n}$, and therefore we know that $\mathcal{C}(\tilde{\mathcal{A}}) / \sim_{lin} \cong \mathbb{Z}^{k-n}$ as well. If we express $A^1(\tilde{\mathcal{A}})$ as a polynomial ring $A_{poly}^1(\tilde{\mathcal{A}})$, we can write

$$A_{poly}^1(\tilde{\mathcal{A}}) \cong \frac{\mathbb{Z}[J_1, \dots, J_{k-n}]}{I_{SR}(\tilde{\mathcal{A}})}. \quad (2.20)$$

We also do not know what the basis elements J_1, \dots, J_{k-n} are in terms of the toric divisor classes D_1, \dots, D_k . However, we can still determine the Chow group using the toric divisor classes and linear equivalence such that

$$A_{poly}^1(\tilde{\mathcal{A}}) \cong \frac{\mathbb{Z}[D_1, \dots, D_k]}{I_{lin} + I_{SR}(\tilde{\mathcal{A}})}. \quad (2.21)$$

By comparing equations (2.11) and (2.16), we see that there is a correspondence⁶ between the columns \mathbf{W}^i of the weight matrix and the toric divisor classes D_i . We may therefore choose a “basis” of divisor classes $\tilde{J}_1, \dots, \tilde{J}_{k-n}$ by picking a set of $k - n$ orthogonal columns of \mathbf{W} . However, this “basis” is not guaranteed to be orthonormal, and will therefore only span $H^{1,1}(\tilde{\mathcal{A}})$ if given rational coefficients. We then say that $\tilde{J}_1, \dots, \tilde{J}_{k-n}$ is a \mathbb{Q} -basis.

Like the weight matrix itself, this \mathbb{Q} -basis is resolution-independent and therefore is valid for all desingularizations $\tilde{\mathcal{A}}$ of \mathcal{A} . This is essential, since it will enable us to accurately compare the Chern classes and intersection numbers of different desingularizations without introducing an arbitrary change of basis. The importance of this property will become clear in Section 2.8.1 when we use Wall’s theorem to glue together the various phases of the complete Kähler cone corresponding to a distinct Calabi–Yau threefold geometry.

Given the toric divisor classes, a \mathbb{Q} -basis of divisor classes, and the linear and Stanley–Reisner ideals, the computation of $A_{poly}^1(\tilde{\mathcal{A}})$ in equation (2.21) is easily accomplished in Sage by defining a PolynomialRing object and an ideal. Because we will be working with a \mathbb{Q} -basis of $H^{1,1}(\tilde{\mathcal{A}})$ rather than a \mathbb{Z} -basis (see Section 2.7), we must define our polynomial ring $A_{poly}^1(\tilde{\mathcal{A}})$ over \mathbb{Q} as follows:

```
sage: C = PolynomialRing(QQ, names=['t']+['D'+str(i+1) for i in range(k)]
+['J'+str(i+1) for i in range(k-n)]);
sage: DD = list(C.gens()[1:-(k-n)]);
sage: JJ = list(C.gens()[-(k-n):]);
sage: ChowIdeal = C.ideal(Ilin+ISR);
```

Again, however, in practice we still do not know the \mathbb{Z} -basis J_1, \dots, J_{k-n} . Later, we will be able to choose one explicitly by considering the Kähler cone constraint (see Section 2.7).

2.6.3 Intersection Numbers

Previously, we computed the Chow group $A_{poly}^1(\tilde{\mathcal{A}})$ as the quotient group of a polynomial ring. However, in this construction, the product of elements can only take the form of polynomials. But as we know, the product of elements of the Chow group is actually an intersection product of 1-cocycles, and not a polynomial product. Moreover, the intersection product of n 1-cocycles on the n -dimensional space $\tilde{\mathcal{A}}$, is just an integer in $A^n(\tilde{\mathcal{A}}) \subset \mathbb{Z}$ (or a rational number in \mathbb{Q} if we have chosen a \mathbb{Q} -basis). Thus, we must choose a normalization for the polynomial ring such that

$$\text{norm} : A_{poly}^n(\tilde{\mathcal{A}}) \xrightarrow{\sim} A^n(\tilde{\mathcal{A}}) \quad (2.22)$$

is a bijection. One such normalization choice involves the lattice volume $\text{vol}(S)$ of a simplex $S \in T(\tilde{\mathcal{A}})$.

⁶In fact, the row space of \mathbf{W} is identical to that of the Mori cone matrix (compare equation (2.11) to the algorithm used to compute the Mori cone matrix in Section 2.7).

If the coordinate patch U has no terminal singularities, i.e., corresponding to points interior to facets on Δ^* (see Section 2.4), then the corresponding simplex S_U has no such interior points, and we say that it is *elementary*. Therefore, because all the cones of a reflexive polytope have lattice distance 1, S_U must have unit volume, $\text{vol}(S_U) = 1$. If, however, the coordinate patch U has terminal (i.e., orbifold) singularities, then there will be points interior to the facets of S_U (see Section 2.4), and the volume of the corresponding simplex will have $\text{vol}(S_U) > 1$.

If $\tilde{\mathcal{A}}$ is smooth everywhere, i.e., has no terminal singularities, then the normalization is simple, and every intersection of n 1-cocycles is equal to 1.

Specifically, we define the normalization as follows. Choose a set of n toric divisor classes $\hat{D}_1, \dots, \hat{D}_n$ such that they have corresponding vertices $\hat{\mathbf{n}}_{i_1}, \dots, \hat{\mathbf{n}}_{i_n} \in \mathcal{P} \cap \hat{S}$ for $\hat{S} \in T(\tilde{\mathcal{A}})$ a simplex. Then, for any set of n toric divisor classes D_{i_1}, \dots, D_{i_n} corresponding to vertices $\mathbf{n}_{i_1}, \dots, \mathbf{n}_{i_n} \in \mathcal{P} \cap S$ for $S \in T(\tilde{\mathcal{A}})$, the normalization takes the form

$$\text{norm} : D_{i_1} \cdot \dots \cdot D_{i_n} \mapsto \frac{1}{\text{vol}(\hat{S})} \frac{D_{i_1} \cdot \dots \cdot D_{i_n}}{\hat{D}_1 \cdot \dots \cdot \hat{D}_n}. \quad (2.23)$$

A Calabi–Yau hypersurface in this construction is defined to be $X = -K_{\tilde{\mathcal{A}}} = \sum_{\rho=1}^k D_{\rho}$ (see Appendix A). Since it is a hypersurface, it has codimension 1, and we can therefore find the intersection numbers in the Chow group $A^n(X)$ by taking $n-1$ toric divisors $D_{i_1}, \dots, D_{i_{n-1}}$, and intersecting them with X directly, i.e., $D_{i_1} \cdot \dots \cdot D_{i_{n-1}} \cdot X$. Because X is a formal sum of toric divisor classes, we can still use the same normalization condition in equation (2.23).

2.6.4 Favorability

It is important to note that the toric divisor classes on $\tilde{\mathcal{A}}$ do not always descend to a Calabi–Yau hypersurface X . In order to visualize this, consider the short exact sequence

$$0 \rightarrow TX \rightarrow T\tilde{\mathcal{A}}|_X \rightarrow \mathcal{N}_{X/\tilde{\mathcal{A}}} \rightarrow 0 \quad (2.24)$$

with dual sequence

$$0 \rightarrow \mathcal{N}_{X/\tilde{\mathcal{A}}}^* \rightarrow T^*\tilde{\mathcal{A}}|_X \rightarrow T^*X \rightarrow 0. \quad (2.25)$$

This induces the long exact sequence in sheaf cohomology, part of which is given by

$$\begin{array}{ccccccc} \dots & \longrightarrow & H^1(X, \mathcal{N}_{X/\tilde{\mathcal{A}}}^*) & \xrightarrow{\alpha} & H^1(X, T^*\tilde{\mathcal{A}}|_X) & \longrightarrow & H^1(X, T^*X) \\ & & & & \searrow & & \\ & & & & & \longleftarrow & \\ & & H^2(X, \mathcal{N}_{X/\tilde{\mathcal{A}}}^*) & \xrightarrow{\beta} & H^2(X, T^*\tilde{\mathcal{A}}|_X) & \longrightarrow & \dots \end{array} \quad (2.26)$$

By Dolbeault’s theorem, $H^1(X, T^*X) \cong H^{1,1}(X) \cong A^1(X)$. Then, by the exactness of equation (2.26), we find

$$A^1(X) \cong \text{coker}(\alpha) \oplus \text{ker}(\beta). \quad (2.27)$$

The cokernel of the map α describes the descent of the Kähler moduli on $\tilde{\mathcal{A}}$ to Kähler moduli on X , while the kernel of the map β describes “new” Kähler moduli on X which do not descend from $\tilde{\mathcal{A}}$. As long as $\text{ker}(\beta) = 0$ and $\text{coker}(\alpha) = H^1(X, T^*\tilde{\mathcal{A}}|_X)$, then all of the Kähler forms descend from the ambient space, and we know $A^1(X)$ completely. Otherwise we are missing important

information about $A^1(X)$. We then say that X , and by a slight abuse of terminology, also the ambient variety $\tilde{\mathcal{A}}$ are *unfavorable*. Studying these unfavorable cases is a problem we leave for future work. In the present study we simply flag these ambient varieties as unfavorable in the database.

If X is favorable then $\dim(A^1(X)) \cong \dim(A^1(\tilde{\mathcal{A}}))$. This is equivalent to $h^{1,1}(X) = \dim(H^{1,1}(X)) \cong \dim(\text{Pic}(\tilde{\mathcal{A}}))$. However, for a toric variety $\text{Pic}(\tilde{\mathcal{A}}) = \mathbb{Z}^{k-n}$. Thus, if $h^{1,1}(X) \neq k - n$, then $\tilde{\mathcal{A}}$ is unfavorable.

2.7 Mori and Kähler Cones

In order to be sure that the hypersurface X is Calabi–Yau, we must ensure that its linear equivalence class $[X]_{lin}$ is a Kähler class, or equivalently that the cohomology class $\gamma(X)$ of its Poincaré dual is a Kähler form. This amounts to determining whether $\gamma(X)$ lies within the Kähler cone

$$\mathcal{K}(\tilde{\mathcal{A}}) = \left\{ \omega \in H^{1,1}(\tilde{\mathcal{A}}) \mid \int_{[C]_{num}} \omega \geq 0, [C]_{num} \in \overline{\text{NE}}(\tilde{\mathcal{A}}) \right\}, \quad (2.28)$$

where $\text{NE}(\tilde{\mathcal{A}}) \subset N_1(\tilde{\mathcal{A}})$ is the Mori cone (or the cone of (numerically effective) curves)

$$\text{NE}(\tilde{\mathcal{A}}) = \left\{ \sum_i a_i [C^i]_{num} \in N_1(\tilde{\mathcal{A}}) \mid a_i \in \mathbb{R}_{>0} \right\} = \text{cone}(\{[C^i]_{num}\}), \quad (2.29)$$

and where $[C^i]_{num}$ are the numerical equivalence classes of the irreducible, proper curves on $\tilde{\mathcal{A}}$. In practice, we specify these curves via their intersections with the toric divisor classes $D_1, \dots, D_k \subset \tilde{\mathcal{A}}$. These intersections form a matrix, which we call the *Mori cone matrix*

$$\mathbf{M}^i_j = [C^i]_{num} \cdot [D_j]_{num} = \int_{[C^i]_{num}} \gamma(D_j). \quad (2.30)$$

Note that the Mori cone itself can be reconstructed from the rows of \mathbf{M} , i.e., $\text{cone}(\{\mathbf{M}^1, \dots, \mathbf{M}^{k-n}\}) \cong \text{NE}(\tilde{\mathcal{A}})$. Then, the rows of \mathbf{M} represent the generating curves $[C^i]_{num}$ of the Mori cone. In order to calculate these, we use an algorithm originally put forward by Oda and Park [49], though the following version is due to Berglund, Katz, and Klemm [53] (see also [54] and [55]):

1. Augment each $\mathbf{n}_\rho \in \mathcal{P}$ to a vector one dimension higher via $\mathbf{n}_\rho \mapsto \bar{\mathbf{n}}_\rho = (1, \mathbf{n}_\rho)$.
2. Find all pairs of n -dimensional simplexes $S_i, S_j \in T(\tilde{\mathcal{A}})$ such that $S_i \cap S_j$ is an $(n - 1)$ -dimensional simplex, and define the set $\mathcal{S} = \{(S_i, S_j)\}$.
3. For each such pair $s \in \mathcal{S}$, find the unique linear relation $\sum_{\rho=1}^k b_\rho^s \cdot \bar{\mathbf{n}}_\rho = 0$, such that
 - 3.1. All the coefficients b_ρ^s are minimal integers.
 - 3.2. $b_\rho^s = 0$ for $\mathbf{n}_\rho \in \mathcal{P} \setminus (S_i \cup S_j)$, where $s = (S_i, S_j)$.
 - 3.3. $b_\rho^s \geq 0$ for $\mathbf{n}_\rho \in (S_i \cup S_j) \setminus (S_i \cap S_j)$, where $s = (S_i, S_j)$.

4. Find a basis of minimal integer vectors $\mathbf{b}^{s_1}, \dots, \mathbf{b}^{s_{k-n}}$ such that \mathbf{b}^s can be expressed as a positive linear combination, for all $s \in \mathcal{S}$.

5. The Mori cone matrix is given by $\mathbf{M} = \begin{pmatrix} (\mathbf{b}^{s_1})^T \\ \vdots \\ (\mathbf{b}^{s_{k-n}})^T \end{pmatrix}$.

We see from equation (2.30) that the rows of \mathbf{M} represent the curves which generate the Mori cone. Next, we compute the matrix dual to \mathbf{M} whose columns generate the Kähler cone. We first choose a basis of divisor classes J_1, \dots, J_{k-n} . We want these to be the generators of the Kähler cone, so from the definition of the Kähler cone in equation (2.28), they must satisfy

$$\int_{[C]_{num}} \gamma(J_j) \geq 0, \quad [C]_{num} \in \overline{\text{NE}}(\tilde{\mathcal{A}}). \quad (2.31)$$

But by the definition of the Mori cone in equation (2.29), we can write

$$\int_{[C]_{num}} \gamma(J_j) = \int_{\sum_i a_i [C^i]_{num}} \gamma(J_j) = \sum_i a_i \cdot \left(\int_{[C^i]_{num}} \gamma(J_j) \right), \quad a_i \in \mathbb{R}_{>0} \quad (2.32)$$

for $[C^i]_{num}$ the curves generating the Mori cone.

We see then that if equation (2.31) is satisfied for the generating curves $[C^i]_{num}$, then it must be satisfied for all $[C]_{num} \in \overline{\text{NE}}(\tilde{\mathcal{A}})$. Thus, we can define the *Kähler cone matrix*

$$\mathbf{K}^i_j = \int_{[C^i]_{num}} \gamma(J_j) \quad \text{with} \quad \mathbf{K} \geq 0. \quad (2.33)$$

But, because J_1, \dots, J_{k-n} form a basis of $A^1(\tilde{\mathcal{A}})$, we require the columns of \mathbf{K} to be orthonormal such that $\mathbf{K}^i_j = \delta^i_j$. Comparing equations (2.30) and (2.33), we can then determine the basis J_1, \dots, J_{k-n} in terms of the toric divisor classes D_1, \dots, D_k . Writing the Mori and Kähler cone matrices in terms of their columns

$$\mathbf{M} = (\mathbf{m}_1 \cdots \mathbf{m}_k) \quad \text{and} \quad \mathbf{K} = (\mathbf{k}_1 \cdots \mathbf{k}_{k-n}), \quad (2.34)$$

we see that

$$J_j = \sum_{i=1}^k b_j^i \cdot D_i \quad \text{when} \quad \mathbf{K}^i_j = \delta^i_j = \sum_{\rho=1}^k b_j^\rho \mathbf{M}^\rho_i. \quad (2.35)$$

There are, in general, many choices of such a basis.

The Lefschetz theorem on (1,1)-classes tells us that $A^1(\tilde{\mathcal{A}}) \cong \text{Pic}(\tilde{\mathcal{A}}) \cong H^{1,1}(\tilde{\mathcal{A}}) \subset H^2(\tilde{\mathcal{A}}, \mathbb{Z})$. Therefore, using the above construction ensures that J_1, \dots, J_{k-n} generate the Kähler cone with integer coefficients (i.e. a \mathbb{Z} -basis). This is an important point if we wish to construct holomorphic line bundles in $\text{Pic}(\tilde{\mathcal{A}})$. Otherwise, however, it is sufficient to construct a basis $\tilde{J}_1, \dots, \tilde{J}_{k-n}$ which generates the Kähler cone with rational coefficients (a \mathbb{Q} -basis). This relaxes the constraint on the columns of \mathbf{K} from orthonormality to orthogonality (see Section 2.6.2). In this case, we can always

choose the basis elements \tilde{J}_i to be a subset of the toric divisor classes and define a modified Kähler cone matrix $\tilde{\mathbf{K}}$ such that

$$\tilde{J}_j = \sum_{i=1}^k \delta_j^i \cdot D_i \quad \text{when} \quad \tilde{\mathbf{K}}_j^i = \sum_{\rho=1}^k \delta_j^\rho \mathbf{M}_\rho^i. \quad (2.36)$$

The Kähler cone matrix $\tilde{\mathbf{K}}$ in this case is no longer orthonormal (only orthogonal), and the Kähler cone itself no longer trivial. \mathbb{Z} - and \mathbb{Q} -bases coincide when $\tilde{\mathcal{A}}$ is smooth (i.e. factorial).

2.8 Gluing of Kähler Cones

We have seen in Section 2.4 that each Gorenstein toric Fano variety \mathcal{A} corresponding to a reflexive polytope in the Kreuzer–Skarke database has at least one, but potentially many MPCP desingularizations $\tilde{\mathcal{A}}$, and that these correspond exactly to FSRT subdivisions of the fan. It is not always the case, however, that these desingularizations contain distinct Calabi–Yau hypersurfaces X . Rather, each desingularization $\tilde{\mathcal{A}}_i$ yields a distinct Kähler cone in the Kähler moduli space within which the Poincaré dual $\gamma(X_i)$ is constrained.

If the Calabi–Yau hypersurfaces of two or more desingularizations share certain key topological invariants, then it can be shown that they are topologically equivalent and can be considered representations of the same Calabi–Yau threefold. In this case, the Kähler form of this Calabi–Yau threefold is allowed to reside within the Kähler cone of either representation, and we refer to these disjoint Kähler cone chambers as its *phases*.

In order to allow the Kähler form to smoothly vary over its full range, the phases of the Kähler cone must be glued together in an appropriate manner. Because the Kähler cone is dual to the Mori cone, this is equivalent to the less intricate task of taking the intersection of the Mori cones corresponding to each Kähler cone phase. This procedure yields a new Mori cone

$$\text{NE}(\tilde{\mathcal{A}}) = \bigcap_i \text{NE}(\tilde{\mathcal{A}}_i). \quad (2.37)$$

The new Mori cone matrix is then given by $\mathbf{M} = \left[\text{rays} \left(\text{NE}(\tilde{\mathcal{A}}) \right) \right]^T$. If the Chow group $A^1(\tilde{\mathcal{A}}_i)$ of each phase is written in the same basis, then by duality the Kähler cone can be determined using either equation (2.35) or (2.36) depending on whether it is a \mathbb{Z} -basis or a \mathbb{Q} -basis (see Sections 2.6.2 and 2.7).

It remains to determine whether some subset of the desingularizations $\tilde{\mathcal{A}}_i$ of \mathcal{A} contain hypersurfaces X_i which are representations of the same Calabi–Yau threefold X . In the next two sections, we present two, presumably equivalent, methods of determining the full, composite Kähler cone corresponding to a distinct Calabi–Yau threefold X .

2.8.1 Chern Classes and Wall’s Theorem

Viewing the Calabi–Yau hypersurfaces X_i as real, $2(n-1)$ -dimensional (in our case $n=4$) oriented manifolds, we may use an influential theorem due to Wall [56]:

Theorem 1. *The homotopy types of complex compact 3-folds are classified by the Hodge numbers, the intersection numbers, and the first Pontryagin class.*

However, because we are working with Calabi–Yau threefolds we can replace the first Pontryagin class with the second Chern class.

The total Chern class of a vector bundle V is given by $c(V) = \sum_i c_i(V)$, where $c_0 = 1$. In the special case that V is actually a line bundle, then $c_1(V)$ is the only non-trivial Chern class, and $c(V) = 1 + c_1(V)$. The splitting principle tells us that we can break up the Chern class of the vector bundles of interest into the product of Chern classes of line bundles. Recall that the Gorenstein toric Fano variety $\tilde{\mathcal{A}}$ has k toric divisors D_1, \dots, D_k , each of which corresponds to a line bundle $\mathcal{O}_{\tilde{\mathcal{A}}}(D_1), \dots, \mathcal{O}_{\tilde{\mathcal{A}}}(D_k)$. As $\tilde{\mathcal{A}}$ is 4-dimensional, its Chern class can be written

$$c(T\tilde{\mathcal{A}}) = 1 + c_1(T\tilde{\mathcal{A}}) + c_2(T\tilde{\mathcal{A}}) + c_3(T\tilde{\mathcal{A}}) + c_4(T\tilde{\mathcal{A}}) \quad (2.38)$$

The Chern classes of the ambient variety $\tilde{\mathcal{A}}$ can be calculated easily in Sage again using the `PolynomialRing` object implemented earlier in Section 2.6.2:

```
sage: cA = prod([(1+C.gen(0)*D) for D in DD]).reduce(ChowIdeal);
sage: cAList = [cA.coefficient({C.gen(0):i})
for i in range(cA.degree(C.gen(0)))];
```

In order to calculate the Chern classes of the Calabi–Yau hypersurface X , we consider the short exact sequence

$$0 \rightarrow TX \rightarrow T\tilde{\mathcal{A}}|_X \rightarrow \mathcal{N}_{X/\tilde{\mathcal{A}}}|_X \cong \mathcal{O}_{\tilde{\mathcal{A}}}(X)|_X = \mathcal{O}_X(X) \rightarrow 0. \quad (2.39)$$

Recall that $c_1(\mathcal{O}_X(X)) = X$. By the definition of the Chern class and because X is 3-dimensional, we write

$$\begin{aligned} c(T\tilde{\mathcal{A}}|_X) &= c(TX) c(\mathcal{O}_X(X)) = \left(1 + c_1(TX) + c_2(TX) + c_3(TX)\right) (1 + X) \\ &= 1 + \left(c_1(TX) + X\right) + \left(c_2(TX) + c_1(TX) X\right) + \left(c_3(TX) + c_2(TX) X\right) + \dots \end{aligned} \quad (2.40)$$

However, the Calabi–Yau condition tells us that $c_1(TX) = 0$ and thus, comparing equations (2.38) and (2.40), we find that $c_1(T\tilde{\mathcal{A}}) = X$ and therefore, after some algebra, that

$$c_2(TX) = c_2(T\tilde{\mathcal{A}}) \quad \text{and} \quad c_3(TX) = c_3(T\tilde{\mathcal{A}}) - c_2(T\tilde{\mathcal{A}}) c_1(T\tilde{\mathcal{A}}). \quad (2.41)$$

Furthermore, the Euler number calculated in Section 2.3 can be checked by integrating the top Chern class

$$\chi(X) = \int_X c_3(TX) \quad (2.42)$$

We now have enough information to compute all of the information required by Wall’s theorem. If these quantities are identical for multiple desingularizations $\tilde{\mathcal{A}}_i$ of \mathcal{A} , then their hypersurfaces X_i should be considered identical and their Kähler cone phases glued via equations (2.37), (2.35), and (2.36).

2.8.2 Identifying Flop Transitions

A presumably⁷ equivalent method of determining when the Kähler cone phases of two desingularizations $\tilde{\mathcal{A}}_i$ should be glued amounts to checking whether or not all singularities in the walls between these phases are avoided by the Calabi–Yau hypersurface. This can be done by tracing a curve with negative self-intersection through a *flop* in the wall of the Kähler cone and making sure that the Calabi–Yau hypersurface misses this curve on both sides.

A curve C with self-intersection $C^2 < 0$ necessarily has negative intersection with every toric divisor which contains it, i.e., $C \cdot D_{j_1} < 0, \dots, C \cdot D_{j_d} < 0$ for $C \subset D_{j_1} \cap \dots \cap D_{j_d}$. If the transition between two phases is a flop, then such a curve C will blow down to a point on the Kähler cone wall, and then blow up again to a new curve C' on the adjacent phase. Then, we can use the following algorithm due to Berglund, Katz, Klemm, and Mayr [57] (see also [54]):

1. Compare the Mori cone matrices \mathbf{M}_1 and \mathbf{M}_2 of two phases corresponding to two desingularizations $\tilde{\mathcal{A}}_1$ and $\tilde{\mathcal{A}}_2$ of \mathcal{A} .

If a row of \mathbf{M}_1 appears in \mathbf{M}_2 with its signs flipped, then these rows represent generators C_1 and C_2 of the Mori cone $NE(\tilde{\mathcal{A}}_1)$ and $NE(\tilde{\mathcal{A}}_2)$, such that C_1 which blows down to a point in the wall of the Kähler cone and then blows up to C_2 on the other side.

Equivalently, there exists a flop from $\tilde{\mathcal{A}}_1$ to $\tilde{\mathcal{A}}_2$.

2. Determine a subvariety $V_1 = D_{i_1} \cap \dots \cap D_{i_d}$ ($d < n$) of $\tilde{\mathcal{A}}_1$ from the intersection of toric divisors which have negative intersection with C_1 (i.e., columns i_1, \dots, i_d of \mathbf{M}_1 with negative entries on the row corresponding to C_1).

Similarly, determine a subvariety $V_2 = D_{i_1} \cap \dots \cap D_{i_d}$ ($d < n$) of $\tilde{\mathcal{A}}_2$ from the intersection of toric divisors which have negative intersection with C_2 (i.e., columns i_1, \dots, i_d of \mathbf{M}_2 with negative entries on the row corresponding to C_2).

3. If $V_1 \cdot X_1 = 0$ and $V_2 \cdot X_2 = 0$, then $X = X_1 = X_2$ is a single Calabi–Yau hypersurface, and the flop does not exist in X .

4. Repeat steps 1 through 3 for all pairs of adjacent Kähler cone phases corresponding to desingularizations of \mathcal{A} .

5. Each group of desingularizations $\{\tilde{\mathcal{A}}_i\}$ which are related by flops that do not exist in the hypersurface defines a single Calabi–Yau geometry X .

The Mori cone of X is obtained by taking the intersection of the Mori cones of the associated desingularizations via equations (2.37).

In practice, however, we have used the gluing procedure based on Wall’s theorem discussed in Section 2.8.1.

⁷We say “presumably” here due to the following issue. Wall’s theorem is enough to ensure that two 3-folds are equivalent as real manifolds. However, it may be that the natural complex structure inherited from the ambient space for two different descriptions of a Calabi–Yau threefold are not in the same connected component of complex structure moduli space.

3 Querying the Database: Illustrative Examples

Max Kreuzer and Harald Skarke have compiled a complete database of all reflexive polytopes in four dimensions. Our aim here is to provide a catalogue of geometrical properties of as many of the associated Calabi–Yau threefold geometries as possible.

The Kreuzer–Skarke database catalogs Newton polytopes which encode the ambient toric varieties in which Calabi–Yau threefolds are embedded as hypersurfaces. Each Newton polytope has a dual, the triangulations of which correspond to separate Calabi–Yau geometries. In this manner, there exists a vastly larger quantity of Calabi–Yau threefolds than reflexive polytopes. Frequently, however, some subset of the triangulations of a dual polytope encode identical topological information, the major difference being the content of the Kähler cone. In such cases, we must treat these as chambers or *phases*, which we “glue together” into a larger Kähler cone corresponding to a single Calabi–Yau geometry.

In the interest of full clarity, the following example database entry will focus on a polytope whose triangulations are divided into two distinct geometries, one of which has a Kähler cone with multiple phases. For those familiar with the Kreuzer–Skarke database, this will be the 95th reflexive polytope in dimension 4 with $h^{1,1} = 3$.

3.1 Search Fields

There are currently two ways to access the database of toric Calabi–Yau threefolds. The first is simple, but limited to a series of text fields and checkboxes, and the second allows the user to enter complex custom querying commands in SQL.

3.1.1 Basic Query

There are many different uses for a database such as this, and therefore we provide a variety of ways to sift through it. The left hand box in Figure 1 allows the user to enter the parameters of the search. The user may choose to specify all, some, or none of the search parameters. In the case that none are specified, entries will be returned in the order in which they were first entered, starting at the beginning of the database. The user may specify a maximum number of matches between 1 and 10,000 for search results. This field is set to 1 by default.

Also, the user may search for multiple values of any field by entering them sequentially in the input box separated by commas. The allowed search fields are:

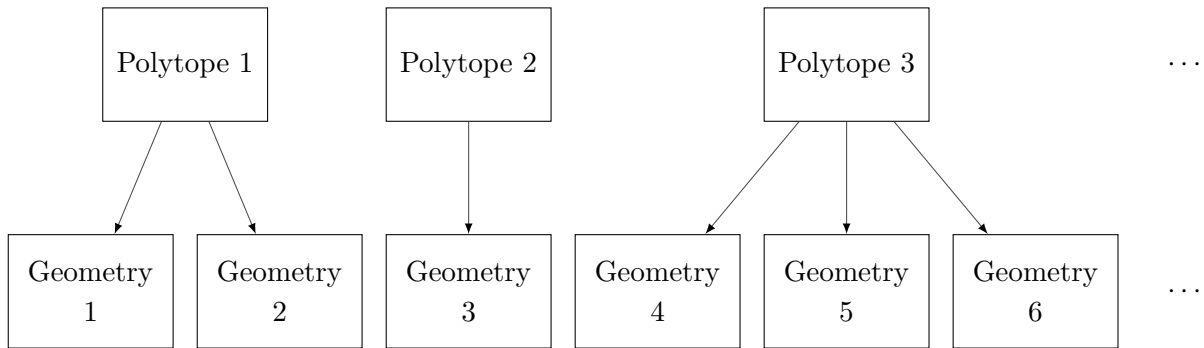
- **ID #**: If this field is specified, at most a single entry will be returned since each Calabi–Yau threefold is indexed with a unique ID. For this reason, **ID #** should not be specified unless the user knows exactly which geometry to isolate.

The next block of fields are all integer-valued:

- **h11**: The Hodge number $h^{1,1} = \dim H^{1,1}(X)$.
- **h21**: The Hodge number $h^{2,1} = \dim H^{2,1}(X)$.

Figure 1: Field-Based Search

- **Euler #**: The Euler number $\chi(X) = 2(h^{1,1} - h^{2,1})$.
- **Polytope #**: The index of a polytope in the Kreuzer–Skarke database for a given value of $h^{1,1}$.
- **Geometry #**: Since each polytope may give rise to multiple Calabi–Yau geometries, we index by these as well, for example in the following way:



- **# of Triangulations**: Recall that triangulations of a polytope which result in identical topological structure must be glued together to form the Kähler cone for that geometry. This

parameter is the number of such triangulations that glue together to form the geometry in question.

The final block of fields are all String-valued and must be enclosed in quotation marks. Each of these must be formatted as a Mathematica matrix (or tensor) with no spaces:

- **Weight Matrix:** This is the weight matrix (see Section 2.5) of the ambient toric variety (viewed as a weighted projective space with multiple sets of weights) in which the Calabi–Yau threefold in question is embedded. Kreuzer and Skarke refer to this in the literature as a CWS or *combined weight system*.

This field will search for matches to weight matrices before and after desingularization of the ambient toric variety.

Note: The rows of the weight matrix must be sorted in ascending order before searching the database.

See Sections 3.2.9 and 3.2.10 for an example of proper formatting.

- **Newton Polytope Vertex Matrix:** This is the matrix of a Newton polytope appearing in the Kreuzer–Skarke database. When searching, its rows and columns must be in the same order as they appear there.

See Section 3.2.6 for an example of proper formatting.

- **Dual Polytope Vertex Matrix:** This is the matrix of the dual to a Newton polytope appearing in the Kreuzer–Skarke database.

Because the ordering of its vertices can be ambiguous, please be sure to sort them (i.e., the columns of the matrix) in ascending order before searching.

See Section 3.2.7 for an example of proper formatting.

- **Dual Polytope Resolved Vertex Matrix:** This is the vertex matrix \mathcal{P} (see Section 2.4) of the dual polytope after subdivision. Some of the vertices given by the columns of this matrix are not necessary to define the convex hull of the polytope, and ignoring them leaves us with the Dual Polytope Vertex Matrix of the previous entry. We call the full set of vertices, including these “extra vertices”, *resolved vertices*.

Again, because the ordering of the non-interior points is ambiguous, please use the Dual Polytope Vertex Matrix augmented on the right by the “extra vertices”, which should be sorted in ascending order (see equation (2.5)).

See Section 3.2.8 for an example of proper formatting.

- **Intersection Polynomial or Tensor:** This is the triple-intersection number tensor, which is a topological invariant of the Calabi–Yau threefold in question. It should be written in Mathematica notation as a nested array of size $h^{1,1} \times h^{1,1} \times h^{1,1}$. Because the intersection tensor is fully symmetric, the ordering is *not* ambiguous in this case, although of course the basis choice can be.

It is also possible to use as input the intersection numbers in polynomial form with divisor class basis elements as variables. However, this introduces unnecessary ambiguities in ordering, and we recommend that the user work with tensors.

See Section 3.2.14 and 3.2.15 for examples of proper formatting in each case.

3.1.2 Advanced Query

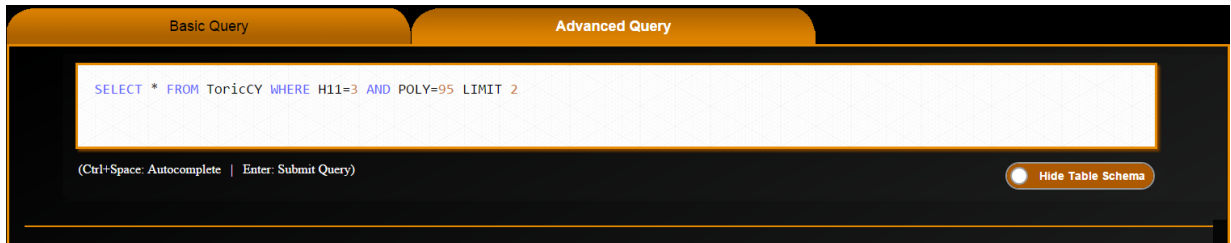


Figure 2: SQL-Based Search

This option provides the user familiar with SQL with a command prompt, allowing him/her to enter a customized query. The above query returns all properties of each total Calabi–Yau geometry corresponding to polytope 95 in the Kreuzer–Skarke list with $h^{1,1} = 3$.

By un toggling the button labelled “Hide Table Schema”, the user may view the available properties and their column names in the SQL table as shown below

Table Name:	ToricCY																			
Column Name:	ID	H11	H21	EULER	POLY	GEOM	FAVORABLE	NVERTS	DVERTS	DPOINTS	CWS	CWSBLOWUP	NTRIANGS	BASIS	TORICDIV	CHERN2	IPOLY	ITENS	MORIMAT	KAHLERMAT
Column Definition:	ToricCY ID #	H11	H21	Euler #	Polytope #	Geometry #	Favorable?	Newton Polytope Vertex Matrix	Dual Polytope Vertex Matrix	Dual Polytope Resolved Vertex Matrix	Weight Matrix	Resolved Weight Matrix	# of Triangulations	Divisor Class Basis	Toric Divisor Classes	2nd Chern Class	Intersection Polynomial	Intersection Tensor	Mori Cone Matrix	Kahler Cone Matrix
Table Name:	ToricCYTriangs																			
Column Name:	ID	PARENTID	TRIANGN	TRIANG	SRIDEAL	CHERNAMB	CHERN3	IPOLYAMB	ITENSAMB	MORIMATN	KAHLERMATN									
Column Definition:	ToricCYTriangs ID #	Corresponding ToricCY ID #	Triangulation #	Triangulation	Stanley-Reisner Ideal	Ambient Chern Classes	3rd Chern Class	Ambient Intersection Polynomial	Ambient Intersection Tensor	Mori Cone Phase Matrix	Kahler Cone Phase Matrix									

Figure 3: Properties and Column Names in SQL Tables

3.2 Search Results for General Calabi–Yau Properties

3.2.1 The Essentials: ID #, H11, H21, and Euler

ID # ▼	H11	H21	Euler #
166	3	81	-156
167	3	81	-156

These four entries will always appear in the results of a database search. **ID #** is the global index within the database of the Calabi–Yau threefold in question.

H11 and **H21** are its Hodge numbers, and **Euler #** is $\chi(X) = 2(h^{1,1} - h^{2,1})$.

** These properties correspond to a particular ambient toric variety, and each embedded geometry will share it.*

The two geometries of polytope 95 with $h^{1,1} = 3$ have database ID numbers 166 and 167. Both geometries have Hodge numbers $h^{1,1} = 3$ and $h^{2,1} = 81$, and Euler number -156 .

3.2.2 Polytope

ID # ▼	H11	H21	Euler #	Polytope #
166	3	81	-156	95
167	3	81	-156	95

The **Polytope #** is the index of a polytope in the Kreuzer–Skarke database for a given value of $h^{1,1}$.

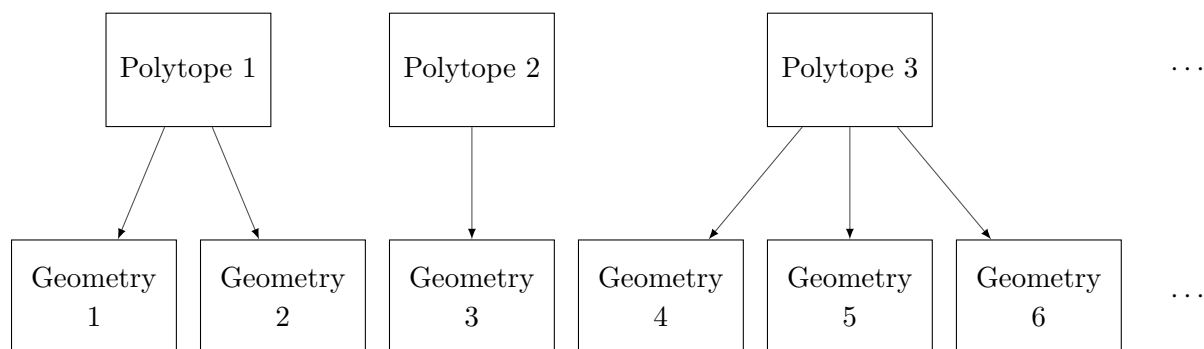
As mentioned, this example uses polytope 95.

** This property corresponds to a particular ambient toric variety, and each embedded geometry will share it.*

3.2.3 Geometry

ID # ▼	H11	H21	Euler #	Geometry #
166	3	81	-156	127
167	3	81	-156	128

The **Geometry #** is the index used to specify a particular Calabi–Yau threefold within the set of geometries of a given $h^{1,1}$. Clusters of these geometries belong to a single polytope in the following way:



In this example, the geometries resulting from polytope 95 in $h^{1,1} = 3$ have ID numbers 166 and 167 within the full database, but geometry numbers 127 and 128 when restricted to the set with $h^{1,1} = 3$.

* This property corresponds to a particular Calabi–Yau threefold geometry.

3.2.4 Is the Geometry Favorable?

ID # ▼	H11	H21	Euler #	Favorable?
166	3	81	-156	1
167	3	81	-156	1

As discussed in Section 2.6.4, we call a Calabi–Yau hypersurfaces *unfavorable* if the ambient space Kähler forms do not descend to provide a basis of $H^{1,1}(X)$. This search parameter is a

Boolean flag which reads 1 for favorable and 0 for unfavorable.

In our example, both geometries 166 and 167 are favorable.

** This property corresponds to a particular Calabi–Yau threefold geometry.*

3.2.5 # of Triangulations

ID # ▼	H11	H21	Euler #	# of Triangulations
166	3	81	-156	2
167	3	81	-156	1

The value of this parameter tells us how many topologically-identical triangulations of the parent polytope had their Kähler cones glued together to form the moduli space of this Calabi–Yau threefold.

In this example, polytope 95 for $h^{1,1} = 3$ has three triangulations, two of which were topologically-equivalent and suitable for gluing. This resulted in the two distinct Calabi–Yau geometries 166 and 167, one of which is composed of two triangulations, and the other of one triangulation.

** This property corresponds to a particular Calabi–Yau threefold geometry.*

3.2.6 Newton Polytope Vertex Matrix

ID # ▼	H11	H21	Euler #	Newton Polytope Vertex Matrix
166	3	81	-156	$\{\{1,1,1,1,-5,-5\},\{0,3,0,0,-6,0\},\{0,0,3,0,0,-6\},\{0,0,0,3,-3,-3\}\}$
167	3	81	-156	$\{\{1,1,1,1,-5,-5\},\{0,3,0,0,-6,0\},\{0,0,3,0,0,-6\},\{0,0,0,3,-3,-3\}\}$

This is the Mathematica-style matrix of a Newton polytope appearing in the Kreuzer–Skarke database. Its rows and columns are given in the same order in which they appear there.

In our example, geometries 166 and 167 both descend from the Newton polytope Δ on the lattice $M \cong \mathbb{Z}^4$ with vertices given by the columns of the matrix

$$[\mathcal{V}(\Delta)] = \begin{pmatrix} 1 & 1 & 1 & 1 & -5 & -5 \\ 0 & 3 & 0 & 0 & -6 & 0 \\ 0 & 0 & 3 & 0 & 0 & -6 \\ 0 & 0 & 0 & 3 & -3 & -3 \end{pmatrix}$$

Note that both Newton polytopes are identical. This is because Δ defines a particular singular toric variety which is resolved to provide the ambient spaces within which both geometries are hypersurfaces.

** This property corresponds to a particular ambient toric variety, and each embedded geometry will share it.*

3.2.7 Dual Polytope Vertex Matrix

ID # ▼	H11	H21	Euler #	Dual Polytope Vertex Matrix
166	3	81	-156	$\{-1,-1,-1,-1,-1,2\},\{0,0,0,1,1,-1\},\{0,0,1,0,1,-1\},\{0,2,0,0,0,-1\}$
167	3	81	-156	$\{-1,-1,-1,-1,-1,2\},\{0,0,0,1,1,-1\},\{0,0,1,0,1,-1\},\{0,2,0,0,0,-1\}$

This is the Mathematica-style matrix of the dual to a Newton polytope Δ appearing in the Kreuzer–Skarke database.

Again, in our example, the dual polytope Δ^* corresponding to geometries 166 and 167 has vertices on the lattice $N \cong \mathbb{Z}^4$ given by the columns of the matrix

$$[\mathcal{V}(\Delta^*)] = \begin{pmatrix} -1 & -1 & -1 & -1 & -1 & 2 \\ 0 & 0 & 0 & 1 & 1 & -1 \\ 0 & 0 & 1 & 0 & 1 & -1 \\ 0 & 2 & 0 & 0 & 0 & -1 \end{pmatrix}$$

Note that the vertices (i.e., the columns of the matrix) are sorted in ascending order.

** This property corresponds to a particular ambient toric variety, and each embedded geometry will share it.*

3.2.8 Dual Polytope Resolved Vertex Matrix

ID # ▼	H11	H21	Euler #	Dual Polytope Resolved Vertex Matrix
166	3	81	-156	$\{-1,-1,-1,-1,-1,2,-1\},\{0,0,0,1,1,-1,0\},\{0,0,1,0,1,-1,0\},\{0,2,0,0,0,-1,1\}$
167	3	81	-156	$\{-1,-1,-1,-1,-1,2,-1\},\{0,0,0,1,1,-1,0\},\{0,0,1,0,1,-1,0\},\{0,2,0,0,0,-1,1\}$

The resolved points \mathcal{P} (see Section 2.4) of the dual polytope Δ^* are those points which are not in the interior region of any cone in the fan of Δ^* . The vertices of Δ^* are examples of non-interior points, but there may be others. These can be thought of as “extra vertices”, which must be taken into account for the purposes of triangulation, but which are redundant in defining the convex hull of Δ^* .

The **Dual Polytope Resolved Vertex Matrix** is just the **Dual Polytope Vertex Matrix** augmented on the right by the “extra vertices”, with the later sorted in ascending order (see equation (2.5)).

In our example, the resolved vertices of the dual polytope Δ^* corresponding to geometries 166 and 167 are given by the columns of the matrix

$$[\mathcal{P}] = \begin{pmatrix} -1 & -1 & -1 & -1 & -1 & 2 & -1 \\ 0 & 0 & 0 & 1 & 1 & -1 & 0 \\ 0 & 0 & 1 & 0 & 1 & -1 & 0 \\ 0 & 2 & 0 & 0 & 0 & -1 & 1 \end{pmatrix}$$

** This property corresponds to a particular ambient toric variety, and each embedded geometry will share it.*

3.2.9 Weight Matrix

ID # ▼	H11	H21	Euler #	Weight Matrix
166	3	81	-156	$\{0,1,1,1,1,2\},\{1,1,0,0,2,2\}$
167	3	81	-156	$\{0,1,1,1,1,2\},\{1,1,0,0,2,2\}$

For each torus action on the ambient variety \mathcal{A} in which a Calabi–Yau threefold is embedded, there is a set of non-negative weights (see Section 2.5) in each of the coordinates which define \mathcal{A} in a manner analogous to weighted projective space. The **Weight Matrix** \mathbf{W} is the matrix for which each row contains the weights for a particular torus action (see equation (2.13)). Kreuzer and Skarke refer to this in the literature as a CWS or *combined weight system*.

In this example, the ambient toric variety corresponding to polytope 95 with $h^{1,1} = 3$ has weight matrix

$$\mathbf{W} = \begin{pmatrix} 0 & 1 & 1 & 1 & 1 & 2 \\ 1 & 1 & 0 & 0 & 2 & 2 \end{pmatrix}$$

Note that there are as many weights in each row as there are vertices in the Dual Polytope Vertex Matrix.

Also, note that the rows of this matrix are sorted in ascending order.

** This property corresponds to a particular ambient toric variety, and each embedded geometry will share it.*

3.2.10 Resolved Weight Matrix

ID # ▼	H11	H21	Euler #	Resolved Weight Matrix
166	3	81	-156	$\{\{0,0,0,0,1,1,1\},\{0,1,1,1,1,2,0\},\{1,1,0,0,2,2,0\}\}$
167	3	81	-156	$\{\{0,0,0,0,1,1,1\},\{0,1,1,1,1,2,0\},\{1,1,0,0,2,2,0\}\}$

The **Weight Matrix \mathbf{W}** describes the ambient toric variety \mathcal{A} corresponding to a polytope in the Kreuzer–Skarke database. However, \mathcal{A} may be singular, and therefore its singularities may need to be resolved to some degree before it can give rise to a smooth Calabi–Yau threefold as a hypersurface. This resolution is performed by blowing up the singular points of \mathcal{A} , resulting in a new ambient variety $\tilde{\mathcal{A}}$ with a new weight matrix $\tilde{\mathbf{W}}$.

In this example, the resolved ambient toric variety corresponds to the weight matrix

$$\tilde{\mathbf{W}} = \begin{pmatrix} 0 & 0 & 0 & 0 & 1 & 1 & 1 \\ 0 & 1 & 1 & 1 & 1 & 2 & 0 \\ 1 & 1 & 0 & 0 & 2 & 2 & 0 \end{pmatrix}$$

Note that there are as many weights in each row as there are non-interior points in the **Dual Polytope Resolved Vertex Matrix**.

Also, note that the rows of this matrix are sorted in ascending order.

** This property corresponds to a particular ambient toric variety, and each embedded geometry will share it.*

3.2.11 Divisor Class Basis

ID # ▼	H11	H21	Euler #	Divisor Class Basis
166	3	81	-156	{{J1,J2,J3},{D2,D4,D5}}
167	3	81	-156	{{J1,J2,J3},{D2,D4,D5}}

Because the Chow group $A^1(X) \cong H^{1,1}(X)$, it must have dimension equal to $h^{1,1}$. Furthermore, since $H^{1,1}(X)$ can be thought of as the vector space of Kähler moduli of the Calabi–Yau threefold X , any divisor class can be written in terms of $h^{1,1}$ independent basis elements (see Section 2.7). Our notation for these basis elements with *real coefficients* is specified here.

In this example, we already know that $h^{1,1} = 3$, so we have the basis elements J_1 , J_2 , and J_3 , which in this case correspond to the three toric divisors D_2 , D_4 , and D_5 (see equation (2.36)).

** This property corresponds to a particular ambient toric variety, and each embedded geometry will share it.*

3.2.12 Toric Divisor Classes

ID # ▼	H11	H21	Euler #	Toric Divisor Classes
166	3	81	-156	{J1-J2,J1,J2,J2,J3,J2+J3,-2*J1+J2+J3}
167	3	81	-156	{J1-J2,J1,J2,J2,J3,J2+J3,-2*J1+J2+J3}

Each of the non-interior points of a dual polytope Δ^* (or edges of its subdivided fan) corresponds to a divisor class in the desingularized ambient toric variety $\tilde{\mathcal{A}}$. We refer to these as the **Toric Divisor Classes**, and we express them in terms of the divisor class basis with real coefficients. Here, we denote each divisor class $[D]_{lin}$ by a representative D .

In this example, the toric divisor classes are given by

$$\begin{aligned}
 D_1 &= J_1 - J_2 & D_2 &= J_1 & D_3 &= J_2 \\
 D_4 &= J_2 & D_5 &= J_3 & D_6 &= J_2 + J_3 \\
 D_7 &= -2J_1 + J_2 + J_3
 \end{aligned}$$

Note that there are as many toric divisor classes as there are columns of the **Dual Polytope**

Resolved Vertex Matrix, and one corresponds to the other in the same order.

** This property corresponds to a particular ambient toric variety, and each embedded geometry will share it.*

3.2.13 2nd Chern Class

ID # ▼	H11	H21	Euler #	2nd Chern Class
166	3	81	-156	$2*J_2^2+12*J_3^2$
167	3	81	-156	$2*J_1*J_3+7*J_2*J_3+3*J_3^2$

This is the 2nd Chern class $c_2(TX)$ specific to the Calabi–Yau threefold X given in terms of the divisor class basis with real coefficients.

In this example, $c_2(TX_{166}) = 2J_2^2 + 12J_3^2$ and $c_2(TX_{167}) = 2J_1J_3 + 7J_2J_3 + 3J_3^2$.

** This property corresponds to a particular Calabi–Yau threefold geometry.*

3.2.14 Intersection Polynomial

ID # ▼	H11	H21	Euler #	Intersection Polynomial
166	3	81	-156	$-3*J_2^3+3*J_1^2*J_3+3*J_1*J_2*J_3+3*J_2^2*J_3+3*J_1*J_3^2+3*J_2*J_3^2+3*J_3^3$
167	3	81	-156	$3*J_1^2*J_3+3*J_1*J_2*J_3+3*J_1*J_3^2+6*J_2*J_3^2$

These are the triple-intersection numbers $\kappa_{ijk}(X)$ specific to the Calabi–Yau threefold X written in the compact polynomial notation

$$P(X) = \sum_{i=1}^{h^{1,1}} \sum_{j=i}^{h^{1,1}} \sum_{k=j}^{h^{1,1}} \kappa_{ijk}(X) J_i J_j J_k$$

In this example, we have

$$\begin{aligned} P(X_{166}) &= -3J_2^3 + 3J_1^2J_3 + 3J_1J_2J_3 + 3J_2^2J_3 + 3J_1J_3^2 + 3J_2J_3^2 + 3J_3^3 \\ P(X_{167}) &= 3J_1^2J_3 + 3J_1J_2J_3 + 3J_1J_3^2 + 6J_2J_3^2 \end{aligned}$$

** This property corresponds to a particular Calabi–Yau threefold geometry.*

3.2.15 Intersection Tensor

ID # ▼	H11	H21	Euler #	Intersection Tensor
166	3	81	-156	{{{0,0,3},{0,0,3},{3,3,3}},{0,0,3},{0,-3,3},{3,3,3}},{3,3,3},{3,3,3},{3,3,3}}}
167	3	81	-156	{{{0,0,3},{0,0,3},{3,3,3}},{0,0,3},{0,0,0},{3,0,6}},{3,3,3},{3,0,6},{3,6,0}}}

These are the triple intersection numbers $\kappa_{ijk}(X)$ specific to the Calabi–Yau threefold X written in tensor form.

In this example, we have

$$\kappa_{1jk}(X_{166}) = \begin{pmatrix} 0 & 0 & 3 \\ 0 & 0 & 3 \\ 3 & 3 & 3 \end{pmatrix}, \quad \kappa_{2jk}(X_{166}) = \begin{pmatrix} 0 & 0 & 3 \\ 0 & -3 & 3 \\ 3 & 3 & 3 \end{pmatrix}, \quad \kappa_{3jk}(X_{166}) = \begin{pmatrix} 3 & 3 & 3 \\ 3 & 3 & 3 \\ 3 & 3 & 3 \end{pmatrix}$$

and

$$\kappa_{1jk}(X_{167}) = \begin{pmatrix} 0 & 0 & 3 \\ 0 & 0 & 3 \\ 3 & 3 & 3 \end{pmatrix}, \quad \kappa_{2jk}(X_{167}) = \begin{pmatrix} 0 & 0 & 3 \\ 0 & 0 & 0 \\ 3 & 0 & 6 \end{pmatrix}, \quad \kappa_{3jk}(X_{167}) = \begin{pmatrix} 3 & 3 & 3 \\ 3 & 0 & 6 \\ 3 & 6 & 0 \end{pmatrix}$$

* This property corresponds to a particular Calabi–Yau threefold geometry.

3.2.16 Mori Cone Matrix

ID # ▼	H11	H21	Euler #	Mori Cone Matrix
166	3	81	-156	{{-1,0,1,1,0,1,1,-3},{1,1,0,0,0,0,-2,0},{1,0,-1,-1,1,0,0,0}}
167	3	81	-156	{{0,0,0,0,1,1,1,-3},{1,1,0,0,0,0,-2,0},{-1,0,1,1,-1,0,0,0}}

This is the Mori cone matrix, the rows of which represent a basis of irreducible, proper curves on $\tilde{\mathcal{A}}$ (see Section 2.7). This matrix \mathbf{M} corresponds to that in equation (2.30).

The Mori cone of the full Calabi–Yau threefold X is the intersection of the Mori cones of its various phases $\tilde{\mathcal{A}}^p$, each corresponding to a distinct triangulation. Each row of $\mathbf{M}_j^i(\tilde{\mathcal{A}}^p)$ represents a basis element of the set $N_1(\tilde{\mathcal{A}}^p)$ of 1-cycles modulo numerical equivalence. We can build up the

Mori cone or “cone of curves” from $M_j^i(\tilde{\mathcal{A}}^p)$, by treating each row as a vertex coordinate in a vector space. Taking the intersection of these cones for all phases p , we can deconstruct it again by treating its extremal rays as the rows of a matrix. Keeping only linearly independent rows, this is now the full Mori cone matrix $M_j^i(X)$ (see Section 2.8).

In our example, geometries 166 and 167 have the following Mori cone matrices

$$M(\tilde{\mathcal{A}}_{166}) = \begin{pmatrix} -1 & 0 & 1 & 1 & 0 & 1 & 1 & -3 \\ 1 & 1 & 0 & 0 & 0 & 0 & -2 & 0 \\ 1 & 0 & -1 & -1 & 1 & 0 & 0 & 0 \end{pmatrix}$$

and

$$M(\tilde{\mathcal{A}}_{167}) = \begin{pmatrix} 0 & 0 & 0 & 0 & 1 & 1 & 1 & -3 \\ 1 & 1 & 0 & 0 & 0 & 0 & -2 & 0 \\ -1 & 0 & 1 & 1 & -1 & 0 & 0 & 0 \end{pmatrix}$$

Note that there is one more column of the Mori cone matrix than columns of the **Dual Polytope Resolved Vertex Matrix**. This is because the final column, in fact, corresponds to the origin and can be ignored for most practical purposes, however it is recorded here for completeness.

** This property corresponds to a particular Calabi–Yau threefold geometry.*

3.2.17 Kähler Cone Matrix

ID # ▼	H11	H21	Euler #	Kähler Cone Matrix
166	3	81	-156	$\{\{0,1,0\},\{1,0,0\},\{0,-1,1\}\}$
167	3	81	-156	$\{\{0,0,1\},\{1,0,0\},\{0,1,-1\}\}$

The requirement that a Calabi–Yau threefold X must be an ample divisor in an ambient toric variety \mathcal{A} puts a strict requirement on the Kähler form ω considered as the Poincaré dual of the divisor class of X . In fact, we find that ω must lie in the Kähler cone (see Section 2.7).

When the geometry is favorable, the $h^{1,1}$ divisor class basis elements J_i of the desingularized ambient toric variety $\tilde{\mathcal{A}}_i$ descend to the Calabi–Yau hypersurface X , so that the Kähler cone is simplicial, and can therefore be expressed via an $h^{1,1} \times h^{1,1}$ matrix of unique intersection numbers $\mathbf{K}(\tilde{\mathcal{A}}_i)$ (see equation (2.33)). However, the Kähler cone will not, in general, be simplicial after gluing multiple phases together and the resultant Kähler cone matrix $\mathbf{K}(\tilde{\mathcal{A}})$ will have at least as many (but potentially more) rows as columns.

When we choose a basis of divisor classes with integer coefficients, the Kähler cone of each phase will be trivial with Kähler cone matrix $\mathbf{K}(\tilde{\mathcal{A}}_i)$ equal to an identity matrix. However, when we choose a basis with real coefficients, this will not always be the case.

Because the **Divisor Class Basis** in this database has real coefficients, the Kähler cone matrix will generally be non-trivial. Furthermore, these matrices are the end result of gluing phases, and will therefore in general have more rows than columns.

In our example, geometries 166 and 167 have the following Kähler cone matrices

$$\mathcal{K}(\tilde{\mathcal{A}}_{166}) = \begin{pmatrix} 0 & 1 & 0 \\ 1 & 0 & 0 \\ 0 & -1 & 1 \end{pmatrix}$$

and

$$\mathcal{K}(\tilde{\mathcal{A}}_{167}) = \begin{pmatrix} 0 & 0 & 1 \\ 1 & 0 & 0 \\ 0 & 1 & -1 \end{pmatrix}$$

** This property corresponds to a particular Calabi–Yau threefold geometry.*

3.3 Search Results for Triangulation-Specific Calabi–Yau Properties

This final set of search results are specific to a particular fine, regular, star triangulation (FSRT) of the dual polytope Δ^* , and are therefore not of much use for most physical calculations. However, they may be instructive in other ways, so we include them.

For each FSRT of the dual polytope Δ^* , there is a unique resolution $\tilde{\mathcal{A}}$ of the singularities of the ambient toric variety \mathcal{A} encoded therein. Each desingularized ambient variety contains an embedded Calabi–Yau hypersurface X . Following Wall’s Theorem, the Hodge numbers $h^{1,1}(X)$ and $h^{2,1}(X)$, the Euler number $\chi(X)$, the intersection tensor $\kappa_{ijk}(X)$, and the second Chern class $c_2(TX)$ are taken to be topological invariants of X . Therefore, any two desingularizations $\tilde{\mathcal{A}}^1$ and $\tilde{\mathcal{A}}^2$ whose Calabi–Yau hypersurfaces X^1 and X^2 have $h^{1,1}(X^1) = h^{1,1}(X^2)$, $h^{2,1}(X^1) = h^{2,1}(X^2)$, $\chi(X^1) = \chi(X^2)$, $\kappa_{ijk}(X^1) = \kappa_{ijk}(X^2)$, and $c_2(X^1) = c_2(X^2)$ are considered to be identical and each of their moduli spaces are taken to be “phases” of the total Calabi–Yau threefold.

In this example search result, both geometries 166 and 167 are constructed from a single dual polytope Δ^* , which has 3 triangulations. Each of these triangulations corresponds to a unique desingularization ($\tilde{\mathcal{A}}_{166}^1$, $\tilde{\mathcal{A}}_{166}^2$, or $\tilde{\mathcal{A}}_{167}$) of the ambient toric variety \mathcal{A} . Furthermore, each desingularized variety has embedded a Calabi–Yau hypersurface (X_{166}^1 , X_{166}^2 , and X_{167}). By Wall’s criteria, X_{166}^1 and X_{166}^2 are topologically equivalent and therefore may be treated as phases of a whole Calabi–Yau geometry X_{166} (geometry 166 in the database). The remaining hypersurface X_{167} therefore constitutes its own Calabi–Yau geometry (geometry 167 in the database).

3.3.1 Triangulation

Within a given geometry, the **Triangulation #** indexes the particular triangulation (and therefore the phase of the moduli space) in question.

In this example, geometry 166 is composed of two triangulations indexed by 1 and 2, and geometry 167 is composed of only one triangulation which has the index 1.

ID # ▼	H11	H21	Euler #	Triangulation #
166	3	81	-156	1
				2
167	3	81	-156	1

3.3.2 Triangulation

ID # ▼	H11	H21	Euler #	Triangulation #	Triangulation
166	3	81	-156	1	{{1,3,5,6},{0,2,3,6},{0,2,5,6},{0,2,3,5},{0,3,5,6},{1,2,5,6},{1,2,3,4},{1,2,3,6},{1,3,4,5},{1,2,4,5},{2,3,4,5}}
166	3	81	-156	2	{{1,3,5,6},{0,2,3,6},{1,2,4,6},{0,2,3,5},{2,3,4,5},{2,3,4,6},{1,2,5,6},{0,3,5,6},{1,3,4,5},{1,2,4,5},{1,3,4,6},{0,2,5,6}}
167	3	81	-156	1	{{0,3,4,6},{1,2,4,6},{0,3,4,5},{1,3,5,6},{0,2,4,6},{1,2,5,6},{0,3,5,6},{1,3,4,5},{1,2,4,5},{0,2,4,5},{1,3,4,6},{0,2,5,6}}

This result tells us precisely how the convex hull of the dual polytope Δ^* is triangulated into simplexes. Each subarray represents a simplex and its contents are the column indices of the **Dual Polytope Resolved Vertex Matrix** which correspond to vertices in \mathcal{P} of the simplex.

These are triangulations of the convex hull boundary of Δ^* , but by placing an extra vertex at the origin $(0, 0, 0, 0)$ in every simplex, they become star triangulations of the full volume of Δ^* .

In our example, both geometries 166 and 167 have **Dual Polytope Resolved Vertex Matrix**

$$[\mathcal{P}] = \begin{pmatrix} \mathbf{0} & \mathbf{1} & \mathbf{2} & \mathbf{3} & \mathbf{4} & \mathbf{5} & \mathbf{6} \\ -1 & -1 & -1 & -1 & -1 & 2 & -1 \\ 0 & 0 & 0 & 1 & 1 & -1 & 0 \\ 0 & 0 & 1 & 0 & 1 & -1 & 0 \\ 0 & 2 & 0 & 0 & 0 & -1 & 1 \end{pmatrix}$$

Then for geometry 166, the first simplex of both its triangulations contains the vertices

$$\{1, 3, 5, 6\} \Rightarrow \left\{ \begin{pmatrix} -1 \\ 0 \\ 0 \\ 2 \end{pmatrix}, \begin{pmatrix} -1 \\ 1 \\ 0 \\ 0 \end{pmatrix}, \begin{pmatrix} 2 \\ -1 \\ -1 \\ -1 \end{pmatrix}, \begin{pmatrix} -1 \\ 0 \\ 0 \\ 1 \end{pmatrix} \right\}$$

And for geometry 167, the first simplex of its single triangulation contains the vertices

$$\{0, 3, 4, 6\} \Rightarrow \left\{ \begin{pmatrix} -1 \\ 0 \\ 0 \\ 0 \end{pmatrix}, \begin{pmatrix} -1 \\ 1 \\ 0 \\ 0 \end{pmatrix}, \begin{pmatrix} -1 \\ 1 \\ 1 \\ 0 \end{pmatrix}, \begin{pmatrix} -1 \\ 0 \\ 0 \\ 1 \end{pmatrix} \right\}$$

3.3.3 Stanley–Reisner Ideal

ID # ▼	H11	H21	Euler #	Triangulation #	Stanley-Reisner Ideal
166	3	81	-156	1	{D1*D2,D1*D5,D5*D7,D2*D3*D4*D6,D3*D4*D6*D7}
166	3	81	-156	2	{D1*D2,D1*D5,D2*D3*D4,D5*D6*D7,D3*D4*D6*D7}
167	3	81	-156	1	{D1*D2,D3*D4,D5*D6*D7}

This is the Stanley–Reisner ideal $I_{\text{SR}}(\tilde{\mathcal{A}})$, a set of maximal ideals corresponding to a specific desingularization of the ambient toric variety $\tilde{\mathcal{A}}$, or equivalently to a specific triangulation of the dual polytope Δ^* . In short, it dictates which subsets of toric divisor classes never intersect at a point.

A toric variety is in general a non-trivial algebraic variety, but it can be understood more concretely as a quotient space of \mathbb{C}^k (minus some exceptional set and where k is given by the number of toric divisor classes) in a construction very similar to that of a simple projective space.

Let \mathbb{C}^k have coordinates (z_1, \dots, z_k) . One of the basic properties of a toric variety $\tilde{\mathcal{A}}$ is that each of its toric divisor classes D_i is given by the subvariety $D_i = \{z_i = 0\}$. If two toric divisor classes never intersect at a point, then the intersection

$$D_1 \cdot D_2 = \int_{\tilde{\mathcal{A}}} D_1 \wedge D_2 \wedge D \wedge E = 0$$

for any arbitrary divisor classes D and E in $\tilde{\mathcal{A}}$, and therefore we find $D_1 \cdot D_2 \in I_{\text{SR}}(\tilde{\mathcal{A}})$. If no other proper subset of $I_{\text{SR}}(\tilde{\mathcal{A}})$ contains $D_1 \cdot D_2$, then it is maximal. In terms of coordinates, $D_1 \cdot D_2$ defines the subvariety $Z(D_1 \cdot D_2)$ by coordinates $(0, 0, z_3, \dots, z_k) \in \mathbb{C}^k$.

Following this procedure, we construct a subvariety $Z(I_i)$ for every maximal ideal $I_i \subset I_{\text{SR}}(\tilde{\mathcal{A}})$. Then, removing the union

$$Z(I_{\text{SR}}(\tilde{\mathcal{A}})) = \bigcup_i Z(I_{\text{SR}})$$

from \mathbb{C}^k ensures that the correct sets of toric divisor classes never intersect at a point.

Then, the desingularized ambient toric variety $\tilde{\mathcal{A}}$ can be written

$$\tilde{\mathcal{A}} \cong \frac{\mathbb{C}^k \setminus Z(I_{\text{SR}}(\tilde{\mathcal{A}}))}{(\mathbb{C}^*)^{k-n} \times \tilde{G}}$$

where the toric group action $(\mathbb{C}^*)^{k-n}$ is defined by the equivalence relations

$$(z_1, \dots, z_k) \sim \left(\lambda \tilde{\mathbf{w}}_i^{-1} z_1, \dots, \lambda \tilde{\mathbf{w}}_i^k z_k \right), \quad \lambda \in \mathbb{C}^*, \forall i = 1, \dots, k - n$$

with \widetilde{W} the **Resolved Weight Matrix**.

In this example, the two triangulations comprising geometry 166 give rise to the Stanley–Reisner ideals

$$I_{\text{SR}}(\widetilde{\mathcal{A}}_{166}^1) = \{D_1 \cdot D_2, D_1 \cdot D_5, D_5 \cdot D_7, D_2 \cdot D_3 \cdot D_4 \cdot D_6, D_3 \cdot D_4 \cdot D_6 \cdot D_7\}$$

$$I_{\text{SR}}(\widetilde{\mathcal{A}}_{166}^2) = \{D_1 \cdot D_2, D_1 \cdot D_5, D_2 \cdot D_3 \cdot D_4, D_5 \cdot D_6 \cdot D_7, D_3 \cdot D_4 \cdot D_6 \cdot D_7\}.$$

The single triangulation comprising geometry 167 gives rise to the Stanley–Reisner ideal

$$I_{\text{SR}}(\widetilde{\mathcal{A}}_{167}) = \{D_1 \cdot D_2, D_3 \cdot D_4, D_5 \cdot D_6 \cdot D_7\}.$$

3.3.4 Ambient Chern Classes

ID # ▼	H11	H21	Euler #	Triangulation #	Ambient Chern Classes
166	3	81	-156	1	{1,3*J2+3*J3,2*J2^2+12*J3^2,-2*J2^3+18*J3^3}
166	3	81	-156	2	{1,3*J2+3*J3,2*J2^2+9*J2*J3+3*J3^2,-2*J2^3+9*J2*J3^2+9*J3^3}
167	3	81	-156	1	{1,3*J2+3*J3,2*J1*J3+7*J2*J3+3*J3^2,-2*J1*J3^2+11*J2*J3^2+4*J3^3}

These are the Chern classes ($c_0(T\widetilde{\mathcal{A}})$, $c_1(T\widetilde{\mathcal{A}})$, $c_2(T\widetilde{\mathcal{A}})$, and $c_3(T\widetilde{\mathcal{A}})$) of a desingularized ambient toric variety $\widetilde{\mathcal{A}}$ given in terms of the divisor class basis. These Chern classes are not invariants associated to the polytope, and are therefore triangulation-specific.

The two triangulations comprising geometry 166 give rise to ambient Chern classes

$$c_0(T\widetilde{\mathcal{A}}_{166}^1) = 1 \qquad c_1(T\widetilde{\mathcal{A}}_{166}^1) = 3J_2 + 3J_3$$

$$c_2(T\widetilde{\mathcal{A}}_{166}^1) = 2J_2^2 + 12J_3^2 \qquad c_3(T\widetilde{\mathcal{A}}_{166}^1) = -2J_2^3 + 18J_3^3$$

and

$$c_0(T\widetilde{\mathcal{A}}_{166}^2) = 1 \qquad c_1(T\widetilde{\mathcal{A}}_{166}^2) = 3J_2 + 3J_3$$

$$c_2(T\widetilde{\mathcal{A}}_{166}^2) = 2J_2^2 + 9J_2J_3 + 3J_3^2 \qquad c_3(T\widetilde{\mathcal{A}}_{166}^2) = -2J_2^3 + 9J_2J_3^2 + 9J_3^3$$

The single triangulation comprising geometry 167 gives rise to ambient Chern classes

$$c_0(T\widetilde{\mathcal{A}}_{167}) = 1 \qquad c_1(T\widetilde{\mathcal{A}}_{167}) = 3J_2 + 3J_3$$

$$c_2(T\widetilde{\mathcal{A}}_{167}) = 2J_1J_3 + 7J_2J_3 + 3J_3^2 \qquad c_3(T\widetilde{\mathcal{A}}_{167}) = -2J_1J_3^2 + 11J_2J_3^2 + 4J_3^3$$

3.3.5 3rd Chern Class

This is the 3rd Chern class $c_3(TX)$ of the Calabi–Yau threefold X . Though it might naively seem from these results like it takes different values on the different phases of X , they can be shown to be identical when taking into account the triple-intersection numbers.

In this example, the two triangulations comprising geometry 166 give rise to

$$c_3(TX_{166}^1) = -8J_2^3 - 6J_2^2J_3 - 36J_2J_3^2 - 18J_3^3$$

ID # ▼	H11	H21	Euler #	Triangulation #	3rd Chern Class
166	3	81	-156	1	$-8*J_2^3-6*J_2^2*J_3-36*J_2*J_3^2-18*J_3^3$
166	3	81	-156	2	$-8*J_2^3-33*J_2^2*J_3-27*J_2*J_3^2$
167	3	81	-156	1	$-6*J_1*J_2*J_3-21*J_2^2*J_3-8*J_1*J_3^2-19*J_2*J_3^2-5*J_3^3$

$$c_3T(X_{166}^2) = -8J_2^3 - 33J_2^2J_3 - 27J_2J_3^2$$

The single triangulation comprising geometry 167 gives rise to

$$c_3(TX_{167}) = -6J_1J_2J_3 - 21J_2^2J_3 - 8J_1J_3^2 - 19J_2J_3^2 - 5J_3^3$$

In all cases, the different products of the J_i are all proportional to the top form on the threefold. Using the intersection numbers to compute the constants of proportionality in each case we find that $c_3(TX)$ is indeed an invariant as it should be. Integrating this over the Calabi–Yau threefold, we obtain the Euler number, -156 in this case

$$\chi(X) = \int_X c_3(TX)$$

3.3.6 Ambient Intersection Polynomial

ID # ▼	H11	H21	Euler #	Triangulation #	Ambient Intersection Polynomial
166	3	81	-156	1	$-1/2*J_1^4-1/2*J_1^3*J_2-1/2*J_1^2*J_2^2-1/2*J_1*J_2^3-3/2*J_2^4+1/2*J_1^3*J_3+1/2*J_1^2*J_2*J_3+1/2*J_1*J_2^2*J_3+1/2*J_1^2*J_3^2+1/2*J_1*J_2*J_3^2+1/2*J_2^2*J_3^2+1/2*J_1*J_3^3+1/2*J_2*J_3^3+1/2*J_3^4$
166	3	81	-156	2	$-J_2^4+J_1^2*J_3^2+J_1*J_2*J_3^2+J_2^2*J_3^2+J_3^4$
167	3	81	-156	1	$J_1^2*J_3^2+J_1*J_2*J_3^2+2*J_2*J_3^3-2*J_3^4$

These are the quadruple intersection numbers $\kappa_{ijkl}(\tilde{\mathcal{A}})$ specific to the desingularized ambient toric variety $\tilde{\mathcal{A}}$ written in the compact polynomial notation

$$P(\tilde{\mathcal{A}}) = \sum_{i=1}^{h^{1,1}} \sum_{j=i}^{h^{1,1}} \sum_{k=j}^{h^{1,1}} \sum_{l=k}^{h^{1,1}} \kappa_{ijkl}(X) J_i J_j J_k J_l$$

In this example, the two triangulations comprising geometry 166 give rise to

$$P(\tilde{\mathcal{A}}_{166}^1) = -\frac{1}{2}J_1^4 - \frac{1}{2}J_1^3J_2 - \frac{1}{2}J_1^2J_2^2 - \frac{1}{2}J_1J_2^3 - \frac{3}{2}J_2^4 + \frac{1}{2}J_1^3J_3 + \frac{1}{2}J_1^2J_2J_3 + \frac{1}{2}J_1J_2^2J_3 + \frac{1}{2}J_2^3J_3 + \frac{1}{2}J_1^2J_3^2 + \frac{1}{2}J_1J_2J_3^2 + \frac{1}{2}J_2^2J_3^2 + \frac{1}{2}J_1J_3^3 + \frac{1}{2}J_2J_3^3 + \frac{1}{2}J_3^4$$

$$P(\tilde{\mathcal{A}}_{166}^2) = -J_2^4 + J_1^2J_3^2 + J_1J_2J_3^2 + J_2^2J_3^2 + J_3^4$$

The single triangulation comprising geometry 167 gives rise to

$$P(\tilde{\mathcal{A}}_{167}) = J_1^2 J_3^2 + J_1 J_2 J_3^2 + 2J_2 J_3^3 - 2J_3^4$$

3.3.7 Ambient Intersection Tensor

ID #	H11	H21	Euler #	Triangulation #	Ambient Intersection Tensor
166	3	81	-156	1	$\{\{-1/2, -1/2, 1/2\}, \{-1/2, -1/2, 1/2\}, \{1/2, 1/2, 1/2\}, \{-1/2, -1/2, 1/2\}, \{-1/2, -1/2, 1/2\}, \{1/2, 1/2, 1/2\}, \{1/2, 1/2, 1/2\}, \{1/2, 1/2, 1/2\}, \{1/2, 1/2, 1/2\}\}$
166	3	81	-156	2	$\{\{0, 0, 0\}, \{0, 0, 0\}, \{0, 0, 1\}, \{0, 0, 0\}, \{0, 0, 0\}, \{0, 0, 1\}, \{0, 0, 1\}, \{0, 0, 1\}, \{1, 1, 0\}\}, \{\{0, 0, 0\}, \{0, 0, 0\}, \{0, 0, 1\}, \{0, 0, 1\}, \{0, 0, 1\}, \{1, 1, 0\}\}, \{\{0, 0, 0\}, \{0, 0, 1\}, \{0, 0, 1\}, \{0, 0, 1\}, \{1, 1, 0\}, \{1, 1, 0\}, \{1, 1, 0\}, \{1, 1, 0\}, \{0, 0, 1\}\}\}$
167	3	81	-156	1	$\{\{0, 0, 0\}, \{0, 0, 0\}, \{0, 0, 1\}, \{0, 0, 0\}, \{0, 0, 0\}, \{0, 0, 1\}, \{0, 0, 1\}, \{0, 0, 1\}, \{1, 1, 0\}\}, \{\{0, 0, 0\}, \{0, 0, 0\}, \{0, 0, 1\}, \{0, 0, 1\}, \{0, 0, 1\}, \{1, 1, 0\}, \{1, 1, 0\}, \{1, 1, 0\}, \{0, 0, 0\}, \{0, 0, 0\}, \{0, 0, 1\}, \{0, 0, 1\}, \{1, 0, 2\}\}, \{\{0, 0, 1\}, \{0, 0, 1\}, \{1, 1, 0\}, \{0, 0, 1\}, \{0, 0, 0\}, \{1, 0, 2\}\}, \{\{1, 1, 0\}, \{1, 0, 2\}, \{0, 2, -2\}\}\}$

These are the quadruple intersection numbers $\kappa_{ijkl}(\tilde{\mathcal{A}})$ specific to the desingularized ambient toric variety $\tilde{\mathcal{A}}$ written in tensor form.

In this example, the two triangulations comprising geometry 166 give rise to

$$\kappa_{11kl}(\tilde{\mathcal{A}}_{166}^1) = \begin{pmatrix} -\frac{1}{2} & -\frac{1}{2} & \frac{1}{2} \\ -\frac{1}{2} & -\frac{1}{2} & \frac{1}{2} \\ \frac{1}{2} & \frac{1}{2} & \frac{1}{2} \end{pmatrix}, \quad \kappa_{22kl}(\tilde{\mathcal{A}}_{166}^1) = \begin{pmatrix} -\frac{1}{2} & -\frac{1}{2} & \frac{1}{2} \\ -\frac{1}{2} & -\frac{3}{2} & \frac{1}{2} \\ \frac{1}{2} & \frac{1}{2} & \frac{1}{2} \end{pmatrix}, \quad \kappa_{33kl}(\tilde{\mathcal{A}}_{166}^1) = \begin{pmatrix} \frac{1}{2} & \frac{1}{2} & \frac{1}{2} \\ \frac{1}{2} & \frac{1}{2} & \frac{1}{2} \\ \frac{1}{2} & \frac{1}{2} & \frac{1}{2} \end{pmatrix}$$

$$\begin{aligned} \kappa_{12kl}(\tilde{\mathcal{A}}_{166}^1) &= \kappa_{21kl}(\tilde{\mathcal{A}}_{166}^1) & \kappa_{13kl}(\tilde{\mathcal{A}}_{166}^1) &= \kappa_{31kl}(\tilde{\mathcal{A}}_{166}^1) & \kappa_{32kl}(\tilde{\mathcal{A}}_{166}^1) &= \kappa_{23kl}(\tilde{\mathcal{A}}_{166}^1) \\ &= \begin{pmatrix} -\frac{1}{2} & -\frac{1}{2} & \frac{1}{2} \\ -\frac{1}{2} & -\frac{1}{2} & \frac{1}{2} \\ \frac{1}{2} & \frac{1}{2} & \frac{1}{2} \end{pmatrix}, & & = \begin{pmatrix} \frac{1}{2} & \frac{1}{2} & \frac{1}{2} \\ \frac{1}{2} & \frac{1}{2} & \frac{1}{2} \\ \frac{1}{2} & \frac{1}{2} & \frac{1}{2} \end{pmatrix}, & & = \begin{pmatrix} \frac{1}{2} & \frac{1}{2} & \frac{1}{2} \\ \frac{1}{2} & \frac{1}{2} & \frac{1}{2} \\ \frac{1}{2} & \frac{1}{2} & \frac{1}{2} \end{pmatrix} \end{aligned}$$

and

$$\kappa_{11kl}(\tilde{\mathcal{A}}_{166}^2) = \begin{pmatrix} 0 & 0 & 0 \\ 0 & 0 & 0 \\ 0 & 0 & 1 \end{pmatrix}, \quad \kappa_{22kl}(\tilde{\mathcal{A}}_{166}^2) = \begin{pmatrix} 0 & 0 & 0 \\ 0 & -1 & 0 \\ 0 & 0 & 1 \end{pmatrix}, \quad \kappa_{33kl}(\tilde{\mathcal{A}}_{166}^2) = \begin{pmatrix} 1 & 1 & 0 \\ 1 & 1 & 0 \\ 0 & 0 & 1 \end{pmatrix}$$

$$\begin{aligned} \kappa_{12kl}(\tilde{\mathcal{A}}_{166}^2) &= \kappa_{21kl}(\tilde{\mathcal{A}}_{166}^2) & \kappa_{13kl}(\tilde{\mathcal{A}}_{166}^2) &= \kappa_{31kl}(\tilde{\mathcal{A}}_{166}^2) & \kappa_{32kl}(\tilde{\mathcal{A}}_{166}^2) &= \kappa_{23kl}(\tilde{\mathcal{A}}_{166}^2) \\ &= \begin{pmatrix} 0 & 0 & 0 \\ 0 & 0 & 0 \\ 0 & 0 & 1 \end{pmatrix}, & & = \begin{pmatrix} 0 & 0 & 1 \\ 0 & 0 & 1 \\ 1 & 1 & 0 \end{pmatrix}, & & = \begin{pmatrix} 0 & 0 & 1 \\ 0 & 0 & 1 \\ 1 & 1 & 0 \end{pmatrix} \end{aligned}$$

The single triangulation comprising geometry 167 gives rise to

$$\begin{aligned} \kappa_{11kl}(\tilde{\mathcal{A}}_{166}^2) &= \begin{pmatrix} 0 & 0 & 0 \\ 0 & 0 & 0 \\ 0 & 0 & 1 \end{pmatrix}, & \kappa_{22kl}(\tilde{\mathcal{A}}_{166}^2) &= \begin{pmatrix} 0 & 0 & 0 \\ 0 & 0 & 0 \\ 0 & 0 & 0 \end{pmatrix}, & \kappa_{33kl}(\tilde{\mathcal{A}}_{166}^2) &= \begin{pmatrix} 1 & 1 & 0 \\ 1 & 0 & 2 \\ 0 & 2 & -2 \end{pmatrix} \\ \kappa_{12kl}(\tilde{\mathcal{A}}_{166}^2) &= \kappa_{21kl}(\tilde{\mathcal{A}}_{166}^2) & \kappa_{13kl}(\tilde{\mathcal{A}}_{166}^2) &= \kappa_{31kl}(\tilde{\mathcal{A}}_{166}^2) & \kappa_{32kl}(\tilde{\mathcal{A}}_{166}^2) &= \kappa_{23kl}(\tilde{\mathcal{A}}_{166}^2) \\ &= \begin{pmatrix} 0 & 0 & 0 \\ 0 & 0 & 0 \\ 0 & 0 & 1 \end{pmatrix}, & & = \begin{pmatrix} 0 & 0 & 1 \\ 0 & 0 & 1 \\ 1 & 1 & 0 \end{pmatrix}, & & = \begin{pmatrix} 0 & 0 & 1 \\ 0 & 0 & 0 \\ 1 & 0 & 2 \end{pmatrix} \end{aligned}$$

3.3.8 Mori Cone Phase Matrix

ID # ▼	H11	H21	Euler #	Triangulation #	Mori Cone Phase Matrix
166	3	81	-156	1	$\{(1,1,0,0,0,-2,0),\{0,-1,-1,-1,0,2,0\},\{-1,0,1,1,0,1,-3\}\}$
166	3	81	-156	2	$\{-1,0,1,1,0,1,-3\},\{1,0,-1,-1,0,0,0\},\{0,1,1,1,-1,0,-2,0\}\}$
167	3	81	-156	1	$\{0,0,0,0,1,1,1,-3\},\{1,1,0,0,0,-2,0\},\{-1,0,1,1,-1,0,0,0\}\}$

This is the Mori cone matrix $\mathcal{M}(\tilde{\mathcal{A}}^p)$ for the p^{th} phase of the desingularized ambient toric variety $\tilde{\mathcal{A}}$.

See Section 3.2.16 for more details about the Mori cone and the construction of the Mori cone matrix.

In this example, the two triangulations comprising geometry 166 give rise to

$$\begin{aligned} \mathcal{M}(\tilde{\mathcal{A}}_{166}^1) &= \begin{pmatrix} 1 & 1 & 0 & 0 & 0 & 0 & -2 & 0 \\ 0 & -1 & -1 & -1 & 1 & 0 & 2 & 0 \\ -1 & 0 & 1 & 1 & 0 & 1 & 1 & -3 \end{pmatrix} \\ \mathcal{M}(\tilde{\mathcal{A}}_{166}^2) &= \begin{pmatrix} -1 & 0 & 1 & 1 & 0 & 1 & 1 & -3 \\ 1 & 0 & -1 & -1 & 1 & 0 & 0 & 0 \\ 0 & 1 & 1 & 1 & -1 & 0 & -2 & 0 \end{pmatrix} \end{aligned}$$

The single triangulation comprising geometry 167 gives rise to

$$\mathcal{M}(\tilde{\mathcal{A}}_{167}) = \begin{pmatrix} 0 & 0 & 0 & 0 & 1 & 1 & 1 & -3 \\ 1 & 1 & 0 & 0 & 0 & 0 & -2 & 0 \\ -1 & 0 & 1 & 1 & -1 & 0 & 0 & 0 \end{pmatrix}$$

Note that because geometry 167 is only composed of a single triangulation, its Mori cone matrix is equivalent to that of the full geometry in Section 3.2.16.

3.3.9 Kähler Cone Phase Matrix

ID # ▼	H11	H21	Euler #	Triangulation #	Kähler Cone Phase Matrix
166	3	81	-156	1	$\{\{1,0,0\},\{-1,-1,1\},\{0,1,0\}\}$
166	3	81	-156	2	$\{\{0,1,0\},\{0,-1,1\},\{1,1,-1\}\}$
167	3	81	-156	1	$\{\{0,0,1\},\{1,0,0\},\{0,1,-1\}\}$

This is the Kähler cone matrix $\mathcal{K}_j^i(\tilde{\mathcal{A}}^p)$ for the p^{th} phase of the desingularized ambient toric variety $\tilde{\mathcal{A}}$.

See Section 3.2.17 for more details about the Kähler cone and the construction of the Kähler cone matrix. Recall that for favorable geometries, the Kähler cone of each phase is simplicial, and therefore these matrices should all be square $h^{1,1} \times h^{1,1}$ matrices. Furthermore, because the **Divisor Class Basis** has real coefficients, these matrices will in general be non-trivial (i.e., not equal to the identity matrix).

In this example, the two triangulations comprising geometry 166 give rise to

$$\mathcal{K}(\tilde{\mathcal{A}}_{166}^1) = \begin{pmatrix} 1 & 0 & 0 \\ -1 & -1 & 1 \\ 0 & 1 & 0 \end{pmatrix}$$

$$\mathcal{K}(\tilde{\mathcal{A}}_{166}^2) = \begin{pmatrix} 0 & 1 & 0 \\ 0 & -1 & 1 \\ 1 & 1 & -1 \end{pmatrix}$$

The single triangulation comprising geometry 167 gives rise to

$$\mathcal{K}(\tilde{\mathcal{A}}_{167}) = \begin{pmatrix} 0 & 0 & 1 \\ 1 & 0 & 0 \\ 0 & 1 & -1 \end{pmatrix}$$

Note that because geometry 167 is only composed of a single triangulation, its Kähler cone matrix is equivalent to that of the full geometry in Section 3.2.17.

4 Discussion

The work described in this paper was motivated primarily by the desire of string theorists for large, easy-to-access, datasets of topological and geometrical properties of Calabi–Yau threefolds. The traditional tool for approaching the largest such set of Calabi–Yau manifolds, the Kreuzer–Skarke database [32], is PALP (Package for Analyzing Lattice Polytopes). PALP is a wonderful resource, but it only goes so far in providing physicists with the information they need.

As an example of this, PALP is unable to compute a secondary polytope that is more than three-dimensional. That is, the triangulation algorithm is coded in such a way as to be limited to polytopes with no more than three points interior to the facets of Δ^* . Therefore, PALP’s ability to triangulate the Kreuzer–Skarke dataset is limited to only the smaller reflexive polytopes. For example, 377 of the 4990 reflexive polytopes with $h^{1,1} = 5$, or 7.6%, could not be triangulated with PALP. At $h^{1,1} = 6$ the fraction of polytopes which could not be triangulated grew to 23.4% (4007 out of 17,101). No polytopes with $h^{1,1} > 6$ which can be triangulated using PALP have been identified.

In addition, and perhaps more importantly, deriving all of the data that a physicist may want from the Kreuzer–Skarke list is computationally intensive. It is a waste of resources for every group interested in such topics to be forced to recompute these results in isolation. Thus, we present our own dataset that we have compiled from the Kreuzer–Skarke database in the online repository located at <http://nuweb1.neu.edu/cydatabase>.

The methods described in Section 2 were applied to the 23,568 polytopes with $h^{1,1} \leq 6$. The number of independent triangulations and glued Calabi–Yau geometries obtained for each value of $h^{1,1}$ is collected in Table 1.

Table 1. Count of Polytopes and Geometries

$h^{1,1}(X)$	2	3	4	5	6	7	8
Number of Polytopes	36	244	1197	4990	17101	50376	128165
Number of Triangulations	48	526	5348	57050	589025*	–	–
Number of Geometries	39	306	2014	13635	85679*	–	–
Number of Favorable Geometries	39	305	2000	13494	84522*	–	–

*Of the 17,101 reflexive polytopes with $h^{1,1} = 6$, we find three cases which each fail to triangulate after 2,160 core-hours of processor time. The numbers in this table reflect the results from the remaining 17,098 polytopes.

The total number of triangulations performed was just under 652,000, resulting in 101,673 CY threefolds. Of these, more than 100,000 are favorable cases, and are thus amenable to meaningful phenomenological study. Where results could be obtained using PALP 2.1, we find agreement between the Sage implementation and the output from PALP.

We note that while the number of polytopes grows polynomially with $h^{1,1}$, the number of core-hours required to obtain the ultimate Calabi–Yau data grows exponentially. A (perhaps naive, but illustrative) fit to the computer time needed for $h^{1,1} \leq 5$ suggests that the processor computation

time spent obeys roughly

$$t = (5 \times 10^{-5}) \times e^{3.5h^{1,1}} \text{ core-hrs} \quad (4.1)$$

For perspective, the extraction of the full set of 85,679 geometries at $h^{1,1} = 6$ took over 113,430 core-hours to complete. This is a little less than 80 core-minutes per unique geometry obtained. To a first approximation, the bulk of the processor time is spent at the triangulation stage, whose computational intensity also grows exponentially.

Work is currently underway to extend these results to $h^{1,1} = 7$ and beyond. If the empirical formula in equation (4.1) continues to hold, this addition will require over 2.2 million core-hours to fully explore. Clearly, extending the database will require mitigating this additional computational load by using the technique of triangulating maximal cones, as described in Section 2.4. As the database expands, the newly-computed Calabi–Yau data will be appended to that already hosted on the web-based repository [33].

Acknowledgements

We are grateful to Lara Anderson, Per Berglund, Volker Braun, Stefan Groot Nibbelink, Benjamin Jurke, Seung-Joo Lee, André Lukas, Herbie Smith, Xin Gao, and Chuang Sun for many helpful discussions during the development of this database. We especially thank Joan Simón for collaboration on a parallel work [58] that applies the database developed in this paper to classify when Calabi–Yau threefolds admit large volume vacua. JG is supported by NSF PHY-1417316. YHH is supported by the Science and Technology Facilities Council, UK, for grant ST/J00037X/1, the Chinese Ministry of Education, for a Chang-Jiang Chair Professorship at NanKai University, and the city of Tian-Jin for a Qian-Ren Award. VJ is supported by the South African Research Chairs Initiative of the Department of Science and Technology and National Research Foundation and thanks McGill University for hospitality. The work of the authors is funded by the U.S. National Science Foundation under the grant CCF-1048082, EAGER: CiC: A String Cartography.

A Extended Glossary of Basic Terms

In the text we give references to the literature for each of the technical steps that we take. In this extended glossary we will describe some of the basic notions which appear in this subject in an informal manner. This is intended to provide the physicist who is familiar with differential geometry, but not the details of algebraic geometry, with a rough guide to several of the concepts which are necessary to follow these technical references. It should be said that in paring down these concepts to provide such a quick introduction to them, we are sacrificing some degree of mathematical rigor.

Divisors:

We will require both of the commonly used descriptions of a divisor on the algebraic variety \mathcal{A} :

- A *Weil divisor* is essentially a formal linear sum of irreducible hypersurfaces within a variety.

$$W = \sum_{\substack{\text{codim}(Y)=1 \\ Y \text{ irred.}}} v_Y \cdot Y . \tag{A.1}$$

- A *Cartier divisor* is a description of a divisor in terms of a collection of rational functions associated to each coordinate patch on a variety: (U_i, f_i) where i runs over the full open cover of \mathcal{A} . On the overlap $U_i \cap U_j$ (for any i and j) it is required that the transition function f_i/f_j is a non-zero rational function. We denote the abelian group of Cartier divisors $\mathcal{C}(\mathcal{A})$.

On smooth varieties, it turns out that the notions of Cartier and Weil divisors coincide. However, since our work will sometimes involve singular spaces we need to keep the two concepts distinct.

We shall also need some other notions associated to the concept of divisors:

- A divisor is said to be *effective* if all of the coefficients v_Y in (A.1) are non-negative, or, in the Cartier case, if the f_i can be chosen to be regular functions.
- A Cartier divisor is said to be *principal* if it is described by a globally-defined rational function.
- Two Cartier divisors D_1 and D_2 are said to be *linearly equivalent* (or more generally, rationally equivalent) if $D_1 = D_2 + D_p$ where D_p is any principal divisor. A complete set of divisors linearly equivalent to D is called a *divisor class* and is denoted⁸ $[D]_{lin}$.
- The intersection of divisors in $[D]_{lin}$ is called its *base locus*. When the base locus is the empty set, we say that the divisor class is *base point free*. Bertini's theorem tells us that a divisor D is smooth away from its base locus, and it is smooth everywhere when $[D]_{lin}$ is base point free.

Chow Ring:

One can define higher codimension generalizations of divisors called algebraic cycles. Just like divisors, there is a notion of rational equivalence of algebraic cycles (a generalization of linear equivalence of divisors), which allows for a concept of cycle classes. We denote the Abelian group of equivalence classes of codimension k cycles on an algebraic variety \mathcal{A} by $A^k(\mathcal{A})$. The Chow ring is then defined by

$$A(\mathcal{A}) = \bigoplus_{k \geq 0} A^k(\mathcal{A}) . \tag{A.2}$$

In particular, the multiplication structure which endows $A(\mathcal{A})$ with the structure of a ring is given by intersection of algebraic cycles. If we have two rational equivalence classes⁹ $[C_1]_{rat}$ and $[C_2]_{rat}$ in $A^i(\mathcal{A})$ and $A^j(\mathcal{A})$ respectively, then we define the product to be $[C_1]_{rat} \cdot [C_2]_{rat} = [C_1 \cap C_2]_{rat}$, which is an element of $A^{i+j}(\mathcal{A})$.

⁸Occasionally in the literature, the set of divisors linearly equivalent to D is called a *linear system* and is denoted $|D|$.

⁹A rational equivalence class is a generalization of a linear equivalence class for cycles of arbitrary codimension.

Line Bundles from Divisors:

Associated to any Cartier divisor D of a variety \mathcal{A} is a holomorphic rank one vector bundle, or *line bundle*, denoted as $\mathcal{O}_{\mathcal{A}}(D)$ over \mathcal{A} . The ratios f_i/f_j which appear in the description of a Cartier divisor above give the transition functions defining $\mathcal{O}_{\mathcal{A}}(D)$.

The Picard group $\text{Pic}(\mathcal{A})$ is the abelian group of isomorphism classes of holomorphic line bundles on \mathcal{A} . There exists a relationship between line bundles and Cartier divisors given by $\text{Pic}(\mathcal{A}) \cong \mathcal{C}/\sim_{lin}$.

- The first Chern class, we write

$$c_1(\mathcal{O}_{\mathcal{A}}(D)) = \gamma(D)$$

where γ represents the operation of Poincaré duality: taking the cohomology class of the $(1, 1)$ -form dual to the divisor class of D .

- If the Cartier divisor D corresponds to a subvariety inside \mathcal{A} , then $\mathcal{O}_{\mathcal{A}}(D)$ is referred to as the *normal bundle* to D in \mathcal{A} .

A line bundle is said to be *very ample* when there are enough global sections to set up an embedding into projective space. Such a globally-generated line bundle always exists in a projective variety. A line bundle is said to be *ample* when some positive power is very ample. By a common abuse of terminology, we sometimes say that the divisor D defining an ample line bundle $\mathcal{O}_{\mathcal{A}}(D)$ is ample as well.

Because global sections must be defined everywhere, they are holomorphic. Therefore, ample Cartier divisors are frequently effective as well.

Adjunction:

Given a divisor D defining a hypersurface in a variety \mathcal{A} there exists a short exact sequence

$$0 \rightarrow TD \rightarrow T\mathcal{A}|_D \rightarrow \mathcal{O}_{\mathcal{A}}(D)|_D \rightarrow 0. \quad (\text{A.3})$$

This essentially says that the tangent directions to the manifold \mathcal{A} at a point on D are those directions tangent to D (encapsulated by TD) and those directions normal to it in \mathcal{A} (encapsulated by the normal bundle $\mathcal{O}_{\mathcal{A}}(D)|_D$).

- Chern classes behave in a particular way under such a short exact sequence. Namely

$$c(T\mathcal{A}|_D) = c(TD) \wedge c(\mathcal{O}_{\mathcal{A}}(D)|_D). \quad (\text{A.4})$$

In particular, therefore, $c_1(TD) = c_1(T\mathcal{A}|_D) - c_1(\mathcal{O}_{\mathcal{A}}(D)|_D) = c_1(T\mathcal{A}|_D) - \gamma(D)$.

Calabi–Yau Manifolds as Hypersurfaces in Fano Varieties:

A Calabi–Yau threefold is a six dimensional Kähler manifold with vanishing first Chern class. We can construct Calabi–Yau manifolds as hypersurfaces D inside an ambient space \mathcal{A} if $c_1(T\mathcal{A}|_D) = c_1(\mathcal{O}_{\mathcal{A}}(D)|_D) = \gamma(D)$. In particular, we can take D to be a so-called *anticanonical divisor* $-K_{\mathcal{A}}$.

- From the tangent bundle $T\mathcal{A}$ we can construct its top wedge power $\mathcal{K}_{\mathcal{A}}^{\vee} = \wedge^{\dim \mathcal{A}} T\mathcal{A}$ which is a line bundle known as the anticanonical bundle.
- By the properties of Chern classes it can be shown that $c_1(T\mathcal{A}) = c_1(\wedge^{\dim \mathcal{A}} T\mathcal{A}) = c_1(\mathcal{K}_{\mathcal{A}}^{\vee})$.
- A Cartier divisor $-K_{\mathcal{A}}$ in the class associated to the anticanonical bundle $\mathcal{K}_{\mathcal{A}}^{\vee}$ is called an anticanonical divisor. In the case where such a divisor defines a codimension one subvariety inside \mathcal{A} we see by adjunction and the above bullet point that this hypersurface has vanishing first Chern class and is thus Calabi–Yau.

The conclusion we reach is that in cases where an anticanonical divisor of a variety \mathcal{A} defines a subvariety of \mathcal{A} , that subvariety is a Calabi–Yau manifold. In other words, $X = -K_{\mathcal{A}}$ is a Calabi–Yau manifold if $-K_{\mathcal{A}}$ is a subvariety of \mathcal{A} . This is always the case when $-K_{\mathcal{A}}$ is ample, which occurs by definition when \mathcal{A} is a *Fano variety*.

Toric Varieties:

A toric variety \mathcal{A} is defined as an algebraic variety containing a torus T as a dense open subset such that the action of T on itself extends to all of \mathcal{A} , i.e., $T \times \mathcal{A} \rightarrow \mathcal{A}$.

An n -dimensional toric variety can be described as a quotient

$$\mathcal{A} \cong \frac{V}{(C^*)^{k-n} \times G}, \quad (\text{A.5})$$

where V is \mathbb{C}^k with some “exceptional set” excised and G is the group of orbifold automorphisms taking \mathcal{A} to itself. In many applications in physics the group G can be taken to be trivial and we are left with the simple split torus action $T = (C^*)^{k-n}$ in the denominator of the quotient.

In a toric variety, the zero locus of each coordinate of V can be associated to a *toric divisor class* $z_i \mapsto D_i = \{z_i = 0\}$, however this map does not take into account linear equivalence. Therefore, the Picard group of holomorphic line bundle classes over \mathcal{A} is lower dimensional. It can be shown that for a toric variety, $\text{Pic}(\mathcal{A}) \cong \mathbb{Z}^{k-n}$.

It is important to note that toric varieties are often singular. This will play a key role in the discussion in the text as we will frequently start with a singular variety and then (partially) resolve it in several different ways.

Gorenstein Toric Fano Varieties and Reflexive Polytopes:

A toric Fano variety is a toric variety with an anticanonical divisor which is an ample Cartier divisor. From the discussion above, this is exactly what we want. In this case, an anticanonical divisor inside a Gorenstein toric Fano variety \mathcal{A} defines a codimension one subvariety $X \subset \mathcal{A}$ which is a Calabi–Yau manifold.

In order for a construction of Calabi–Yau manifolds to have substantial computational power, we must be able to determine the relevant quantities of these manifolds using combinatorics and linear algebra. Happily, this is possible in the Gorenstein toric case due to the one-to-one correspondence between Gorenstein toric Fano varieties and reflexive polytopes.

- A lattice polytope Δ is the convex hull of finitely many vertices on an integer lattice $M \cong \mathbb{Z}^n$.
- We then define a dual lattice $N \cong \mathbb{Z}^n$ parameterized by the maps taking the M into the integers, i.e., $N = \text{Hom}_{\mathbb{Z}}(M, \mathbb{Z})$.
- Then, on N , we can define the dual (or polar) polytope by

$$\Delta^* = \{\mathbf{n} \in N \mid \langle \mathbf{m}, \mathbf{n} \rangle \geq -1, \forall \mathbf{m} \in \Delta\} . \quad (\text{A.6})$$

- A lattice polytope $\Delta \subset M$ containing only the origin of M in its interior is said to be *reflexive* if $\Delta^* \subset N$ is also a lattice polytope containing only the origin of N in its interior.
- Such reflexive polytopes are in one-to-one correspondence (up to birational equivalence) with Gorenstein toric Fano varieties. In particular, we can derive many properties of such varieties from simple combinatorial operations involving the polytope.

Below we give an example of how information about a Gorenstein toric Fano variety \mathcal{A} can be extracted from the data of a polytope. In particular, we will briefly describe how one obtains some information about divisors in \mathcal{A} .

Divisors From Polytopes:

A heuristic description of how one extracts information about divisors given a polytope Δ^* is as follows

- For each point $\mathbf{m} \in \Delta$, define the *supporting hyperplane* $H_{\mathbf{m}} = \{\mathbf{n} \in N \mid \langle \mathbf{m}, \mathbf{n} \rangle = -1\}$. Then, by equation (A.6), we see that Δ^* is bounded by the hyperplanes $H_{\mathbf{m}}$.
- Then, a *facet*, or $(n - 1)$ -dimensional face of Δ^* , is given by $F = \Delta^* \cap H$ for H a supporting hyperplane. We define the set \mathcal{F} of facets and all their intersections. Then, the subset of $(d - 1)$ -dimensional faces is denoted \mathcal{F}_{d-1} .
- We define the $(d - 1)$ -skeleton skel_{d-1} to be the union of faces of dimension $\leq d - 1$.
- A d -dimensional convex, rational, polyhedral *cone* is given by $\sigma = \text{cone}(F)$ for $F \in \mathcal{F}_{d-1}$, where $\text{cone}(F)$ is the set of all rays that pass from the origin through points in F . The n -dimensional cones are called *maximal cones*, and we define the set Σ , called the *fan* of Δ^* , of maximal cones and all their intersections. Then, the subset of d -dimensional cones is denoted Σ_d , and their union $|\Sigma_d| = \bigcup_{\sigma \in \Sigma_d} \sigma$ is called the *d-support* of Δ^* .
- One-dimensional rays (or more precisely primitive generators of Σ_1) in this fan correspond one-to-one with divisors on the Gorenstein toric Fano variety \mathcal{A} . These are just the toric divisor classes, denoted by D_i .
- A Calabi–Yau hypersurface, defined by the anticanonical divisor of the Gorenstein toric Fano variety, can then be written in terms of the toric divisor classes

$$X = -K_{\mathcal{A}} = \sum_i D_i . \quad (\text{A.7})$$

- A generic Calabi–Yau hypersurface can also be written in terms of the vanishing of a homogeneous Laurent polynomial $P_X(\mathbf{z})$ by

$$P_X(\mathbf{z}) = \sum_{\mathbf{m} \in \Delta \cap M} c_{\mathbf{m}} \prod_i z_i^{\langle \mathbf{m}, \mathbf{n}_i \rangle + 1}, \quad (\text{A.8})$$

where $c_{\mathbf{m}}$ are arbitrary coefficients, the choice of which is related to the complex structure on X . Because the exponents of the monomial terms are related to the points of the polytope Δ , we sometimes refer to it as a *Newton polytope*.

B Nomenclature

Some of the mathematical background which is required in this work is reviewed in simple terms in Appendix A. Here, we define some of the notation which appears in the main discussion of this paper.

- \mathcal{A} is an ambient Gorenstein toric Fano variety.
- Δ is a reflexive Newton polytope corresponding to the ambient variety \mathcal{A} .
- The desingularization of \mathcal{A} is $\tilde{\mathcal{A}}$.
- $\mathcal{V}(\Delta^*)$ is the set of vertices of the reflexive polytope Δ^* before subdividing.
- \mathcal{P} is the set of vertices of Δ^* after subdividing.
- $M \cong \text{Hom}(T, \mathbb{C}^*) \cong \mathbb{Z}^n$ is the character lattice of the split torus $T = (\mathbb{C}^*)^{k-n}$.
- $N \cong \text{Hom}(M, \mathbb{Z}) \cong \mathbb{Z}^n$ is the dual lattice.
- $\langle \cdot, \cdot \rangle : M \times N \rightarrow \mathbb{Z}$ is the inner product between dual lattices.
- $\text{card}(P)$ is the cardinality, or number of lattice points, in any subspace $P \subset M$ or N .
- In this paper, we use $n = \dim(\mathcal{A}) = \dim(\tilde{\mathcal{A}})$, $k = \text{card}(\mathcal{P})$, and d an arbitrary dimension.
- $\text{relint}(P)$ is the relative interior of any subspace $P \subset M$ or N and ∂P is its boundary.
- $[P]$ is the $n \times \text{card}(P)$ matrix with columns given by the vectors $\mathbf{p} \in P$ for P some point configuration.
- Occasionally, for the sake of organization and reproducibility, we will use $\text{sort}(P)$ to signify the poset of lattice points in a subspace $P \subset M$ or N , sorted in ascending order by their coordinate values in M or N .
- $H_{\mathbf{m}}(\Delta^*) = \{\mathbf{n} \in N \mid \langle \mathbf{m}, \mathbf{n} \rangle = -1\}$ is a supporting hyperplane of Δ^* corresponding to the point $\mathbf{m} \in \Delta$.
- $\Delta^* = \{\mathbf{n} \in N \mid \langle \mathbf{m}, \mathbf{n} \rangle \geq -1, \forall \mathbf{m} \in \Delta\}$ is the dual (or polar) polytope, which is also equal to the intersection of half-spaces bounded by the $H_{\mathbf{m}}(\Delta^*)$, $\mathbf{m} \in \Delta$.

- The faces $F \in \mathcal{F}(\Delta^*)$ of Δ^* are formed by all possible intersections of the supporting hyperplanes $H_{\mathbf{m}}(\Delta^*)$, $\mathbf{m} \in \Delta$ with Δ^* . The subset of $(d-1)$ -faces $\mathcal{F}_{d-1}(\Delta^*) \subset \mathcal{F}(\Delta^*)$ is the set of $(d-1)$ -dimensional faces.
- The $(d-1)$ -skeleton skel_{d-1} is the union of faces F of dimension $\leq d-1$. We see that $\mathcal{V}(\Delta^*) = \text{skel}_0(\Delta^*)$.
- For each face $F \in \mathcal{F}(\Delta^*)$, there is a corresponding dual face $F^* \in \mathcal{F}(\Delta)$ given by $F^* = \{\mathbf{m} \in \Delta \mid H_{\mathbf{m}}(\Delta^*) \cap F \neq \emptyset\}$.
- For every face $F \in \mathcal{F}(\Delta^*)$, there is a corresponding convex rational polyhedral cone $\sigma_F = \text{cone}(F)$ formed by the space of rays from the origin passing through F .
- $\text{rays}(\sigma)$ is the set of extremal rays of the convex, polyhedral cone σ . Note that $\text{cone}(\text{rays}(\sigma)) = \sigma$.
- $\Sigma(\Delta^*) = \{\sigma_F \mid F \in \mathcal{F}(\Delta^*)\}$ is the fan of Δ^* . The subset of d -cones is $\Sigma_d(\Delta^*) = \{\sigma_F \mid F \in \mathcal{F}_{d-1}(\Delta^*)\}$.
- For each cone $\sigma \in \Sigma(\Delta^*)$, there is a corresponding dual cone $\sigma^* \in \Sigma(\Delta)$ given by $\sigma^* = \{\mathbf{m} \in M \mid \langle \mathbf{m}, \mathbf{n} \rangle \geq 0, \mathbf{n} \in \sigma\}$.
- $T(\tilde{\mathcal{A}})$ is the triangulation of Δ^* corresponding to the desingularization $\tilde{\mathcal{A}}$ of \mathcal{A} . The set of all such triangulations is \mathcal{T} .
- $\text{vol}(S)$ is the lattice volume of a simplex $S \in T(\tilde{\mathcal{A}})$, defined to be the geometric, oriented volume of S divided by the volume $1/n!$ of a unit simplex [59].
- $\mathcal{U}(\tilde{\mathcal{A}}) = \{U \subset \tilde{\mathcal{A}} \mid \tilde{\mathcal{A}} \cong \bigcup U\}$ is an open cover of $\tilde{\mathcal{A}}$.
- D_1, \dots, D_k are toric divisor classes on $\tilde{\mathcal{A}}$, and J_1, \dots, J_{k-n} are the basis elements of the space of divisor classes on $\tilde{\mathcal{A}}$.
- Vertices $\mathbf{m}_U \in \mathcal{V}(\Delta)$, facets $F_U \in \mathcal{F}_{n-1}(\Delta^*)$, and maximal cones in $\sigma_U \in \Sigma(\Delta^*)$ are each in one-to-one correspondence with coordinate patches $U \in \mathcal{U}(\tilde{\mathcal{A}})$ with bijections $\mathbf{m}_U \rightarrow U$, $F_U \rightarrow U$, and $\sigma_U \rightarrow U$.

References

- [1] M. Kreuzer and H. Skarke, “Complete classification of reflexive polyhedra in four-dimensions,” *Adv. Theor. Math. Phys.* **4**, 1209 (2002) [[hep-th/0002240](#)].
- [2] T. Kaluza, “On the Problem of Unity in Physics,” *Sitzungsber. Preuss. Akad. Wiss. Berlin (Math. Phys.)* **1921**, 966 (1921).
- [3] O. Klein, “Quantum Theory and Five-Dimensional Theory of Relativity. (In German and English),” *Z. Phys.* **37**, 895 (1926) [*Surveys High Energ. Phys.* **5**, 241 (1986)].

- [4] P. Candelas, G. T. Horowitz, A. Strominger and E. Witten, “Vacuum Configurations for Superstrings,” Nucl. Phys. B **258**, 46 (1985).
- [5] V. Braun, Y. H. He, B. A. Ovrut and T. Pantev, “A Heterotic standard model,” Phys. Lett. B **618**, 252 (2005) [[hep-th/0501070](#)].
- [6] V. Braun, Y. H. He, B. A. Ovrut and T. Pantev, “A Standard model from the $E(8) \times E(8)$ heterotic superstring,” JHEP **0506**, 039 (2005) [[hep-th/0502155](#)].
- [7] V. Bouchard and R. Donagi, “An $SU(5)$ heterotic standard model,” Phys. Lett. B **633**, 783 (2006) [[hep-th/0512149](#)].
- [8] V. Braun, Y. H. He, B. A. Ovrut and T. Pantev, “The Exact MSSM spectrum from string theory,” JHEP **0605**, 043 (2006) [[hep-th/0512177](#)].
- [9] L. B. Anderson, J. Gray, Y. H. He and A. Lukas, “Exploring Positive Monad Bundles And A New Heterotic Standard Model,” JHEP **1002**, 054 (2010) [[arXiv:0911.1569](#) [hep-th]].
- [10] L. B. Anderson, J. Gray, A. Lukas and E. Palti, “Heterotic Line Bundle Standard Models,” JHEP **1206**, 113 (2012) [[arXiv:1202.1757](#) [hep-th]].
- [11] T. Hubsch, “Calabi-yau Manifolds: Motivations and Constructions,” Commun. Math. Phys. **108**, 291 (1987).
- [12] P. Candelas, A. M. Dale, C. A. Lutken and R. Schimmrigk, “Complete Intersection Calabi-Yau Manifolds,” Nucl. Phys. B **298**, 493 (1988).
- [13] P. Green and T. Hubsch, “Calabi-yau Manifolds as Complete Intersections in Products of Complex Projective Spaces,” Commun. Math. Phys. **109**, 99 (1987).
- [14] P. Candelas, C. A. Lutken and R. Schimmrigk, “Complete Intersection Calabi-yau Manifolds. 2. Three Generation Manifolds,” Nucl. Phys. B **306**, 113 (1988).
- [15] I. Brunner, M. Lynker and R. Schimmrigk, “Unification of M theory and F theory Calabi-Yau fourfold vacua,” Nucl. Phys. B **498**, 156 (1997) [[hep-th/9610195](#)].
- [16] J. Gray, A. S. Haupt and A. Lukas, “All Complete Intersection Calabi-Yau Four-Folds,” JHEP **1307**, 070 (2013) [[arXiv:1303.1832](#) [hep-th]].
- [17] J. Gray, A. S. Haupt and A. Lukas, “Topological Invariants and Fibration Structure of Complete Intersection Calabi-Yau Four-Folds,” JHEP **1409**, 093 (2014) [[arXiv:1405.2073](#) [hep-th]].
- [18] D. R. Morrison and W. Taylor, “Toric bases for 6D F-theory models,” Fortsch. Phys. **60**, 1187 (2012) [[arXiv:1204.0283](#) [hep-th]].
- [19] L. B. Anderson and W. Taylor, “Geometric constraints in dual F-theory and heterotic string compactifications,” JHEP **1408**, 025 (2014) [[arXiv:1405.2074](#) [hep-th]].
- [20] M. Kreuzer and H. Skarke, “Reflexive polyhedra, weights and toric Calabi-Yau fibrations,” Rev. Math. Phys. **14**, 343 (2002) [[math/0001106](#) [math-ag]].

- [21] P. Berglund and T. Hubsch, “A Generalized construction of mirror manifolds,” Nucl. Phys. B **393**, 377 (1993) [[hep-th/9201014](#)].
- [22] R. Blumenhagen, X. Gao, T. Rahn and P. Shukla, “A Note on Poly-Instanton Effects in Type IIB Orientifolds on Calabi-Yau Threefolds,” JHEP **1206**, 162 (2012) [[arXiv:1205.2485](#) [hep-th]].
- [23] X. Gao and P. Shukla, “On Classifying the Divisor Involutions in Calabi-Yau Threefolds,” JHEP **1311**, 170 (2013) [[arXiv:1307.1139](#) [hep-th]].
- [24] X. Gao and P. Shukla, “F-term Stabilization of Odd Axions in LARGE Volume Scenario,” Nucl. Phys. B **878**, 269 (2014) [[arXiv:1307.1141](#) [hep-th]].
- [25] M. Cicoli, S. Krippendorf, C. Mayrhofer, F. Quevedo and R. Valandro, “D-Branes at del Pezzo Singularities: Global Embedding and Moduli Stabilisation,” JHEP **1209**, 019 (2012) [[arXiv:1206.5237](#) [hep-th]].
- [26] M. Cicoli, M. Kreuzer and C. Mayrhofer, “Toric K3-Fibred Calabi-Yau Manifolds with del Pezzo Divisors for String Compactifications,” JHEP **1202**, 002 (2012) [[arXiv:1107.0383](#) [hep-th]].
- [27] M. Cicoli, J. P. Conlon and F. Quevedo, “General Analysis of LARGE Volume Scenarios with String Loop Moduli Stabilisation,” JHEP **0810**, 105 (2008) [[arXiv:0805.1029](#) [hep-th]].
- [28] M. Cicoli, D. Klevers, S. Krippendorf, C. Mayrhofer, F. Quevedo and R. Valandro, “Explicit de Sitter Flux Vacua for Global String Models with Chiral Matter,” JHEP **1405**, 001 (2014) [[arXiv:1312.0014](#) [hep-th]].
- [29] V. Batyrev and M. Kreuzer, “Integral cohomology and mirror symmetry for Calabi-Yau 3-folds,” [[math/0505432](#) [math-ag]].
- [30] V. V. Batyrev, “Dual polyhedra and mirror symmetry for Calabi-Yau hypersurfaces in toric varieties,” J. Alg. Geom. **3**, 493 (1994) [[alg-geom/9310003](#)].
- [31] M. Kreuzer and H. Skarke, “PALP: A Package for analyzing lattice polytopes with applications to toric geometry,” Comput. Phys. Commun. **157**, 87 (2004) [[math/0204356](#) [math-sc]].
- [32] M. Kreuzer and H. Skarke, Calabi-Yau data, <http://hep.itp.tuwien.ac.at/~kreuzer/CY/>
- [33] R. Altman, Toric Calabi-Yau Threefold Database, <http://nuweb1.neu.edu/cydatabase/>
- [34] A. P. Braun and N. O. Walliser, “A New offspring of PALP,” [[arXiv:1106.4529](#) [math.AG]].
- [35] Y. H. He, S. J. Lee and A. Lukas, “Heterotic Models from Vector Bundles on Toric Calabi-Yau Manifolds,” JHEP **1005**, 071 (2010) [[arXiv:0911.0865](#) [hep-th]].
- [36] Y. H. He, M. Kreuzer, S. J. Lee and A. Lukas, “Heterotic Bundles on Calabi-Yau Manifolds with Small Picard Number,” JHEP **1112**, 039 (2011) [[arXiv:1108.1031](#) [hep-th]].
- [37] Y. H. He, S. J. Lee, A. Lukas and C. Sun, “Heterotic Model Building: 16 Special Manifolds,” JHEP **1406**, 077 (2014) [[arXiv:1309.0223](#) [hep-th]].

- [38] A. P. Braun, J. Knapp, E. Scheidegger, H. Skarke and N. O. Walliser, “PALP - a User Manual,” [arXiv:1205.4147 [math.AG]].
- [39] W. A. Stein et al., *Sage Mathematics Software (Version 5.12)*, The Sage Development Team, 2013, <http://www.sagemath.org>.
- [40] V. Braun, J. Whitney, and M. Hampton, Triangulations of a point configuration, http://www.sagemath.org/doc/reference/geometry/sage/geometry/triangulation/point_configuration.html
- [41] Matsuki, K. (2002). *Introduction to the Mori program*. Springer.
- [42] Cutkosky, S. (1988). Elementary contractions of Gorenstein threefolds. *Mathematische Annalen*, 280(3), 521-525.
- [43] Gross, M., Huybrechts, D., and Joyce, D. (Eds.). (2003). *Calabi-Yau Manifolds and Related Geometries: Lectures at a Summer School in Nordfjordeid, Norway, June, 2001*. Springer.
- [44] Gelfand, I. M., Kapranov, M. M., and Zelevinsky, A. Discriminants, Resultants and Multidimensional Determinants, 1994. *Birkahuser, Boston Zbl0827, 14036*.
- [45] Lee, C. W. (1990). Regular triangulations of convex polytopes.
- [46] Thomas, R. R. (2006). *Lectures in geometric combinatorics* (Vol. 33). American Mathematical Soc..
- [47] Haase, C. and Nill, B. (2008). Lattices generated by skeletons of reflexive polytopes. *Journal of Combinatorial Theory, Series A*, 115(2), 340-344.
- [48] Nill, B. (2006). Complete toric varieties with reductive automorphism group. *Mathematische Zeitschrift*, 252(4), 767-786.
- [49] Oda, T. (1985). *Convex bodies and Algebraic Geometry, An Introduction to the Theory of Toric Varieties*, A Series of Modern Surveys in Mathematics.
- [50] Jörg Rambau. *TOPCOM: Triangulations of Point Configurations and Oriented Matroids*, Mathematical Software - ICMS 2002 (Cohen, Arjeh M. and Gao, Xiao-Shan and Takayama, Nobuki, eds.), World Scientific (2002), pp. 330-340
- [51] C. Long, L. McAllister and P. McGuirk, “Heavy Tails in Calabi-Yau Moduli Spaces,” [arXiv:1407.0709 [hep-th]].
- [52] Billera, L. J., Filliman, P., and Sturmfels, B. (1990). Constructions and complexity of secondary polytopes. *Advances in Mathematics*, 83(2), 155-179.
- [53] P. Berglund, S. H. Katz and A. Klemm, “Mirror symmetry and the moduli space for generic hypersurfaces in toric varieties,” *Nucl. Phys. B* **456**, 153 (1995) [[hep-th/9506091](http://arxiv.org/abs/hep-th/9506091)].
- [54] T. W. Grimm and H. Hayashi, “F-theory fluxes, Chirality and Chern-Simons theories,” *JHEP* **1203**, 027 (2012) [arXiv:1111.1232 [hep-th]].

- [55] S. Reffert, “The Geometer’s Toolkit to String Compactifications,” arXiv:0706.1310 [hep-th].
- [56] Wall, C. T. C. (1966). Classification problems in differential topology. V. *Inventiones mathematicae*, 1(4), 355-374.
- [57] P. Berglund, S. H. Katz, A. Klemm and P. Mayr, “New Higgs transitions between dual N=2 string models,” Nucl. Phys. B **483**, 209 (1997) [[hep-th/9605154](#)].
- [58] R. Altman, J. Gray, Y. He, V. Jejjala, B. Nelson, and J. Simon (2014). Manuscript in preparation.
- [59] J. Knapp and M. Kreuzer, “Toric Methods in F-theory Model Building,” Adv. High Energy Phys. **2011**, 513436 (2011) [[arXiv:1103.3358](#) [hep-th]].